MARIA S.MERIAN Berichte

Einsetzen und Modifikation in Pfaden und Intensitäten des Wassermassenaustauschs zwischen dem südöstlichen Pazifik und dem Südatlantik mit Fokus auf dem Falkland Plateau, nördlichen Scotia Bogen und West Georgia Becken

Cruise No. MSM 81

2.2.2019-15.3.2019,

Valparaiso (Chile) – Montevideo (Uruguay)

Falkland Sediment Drifts

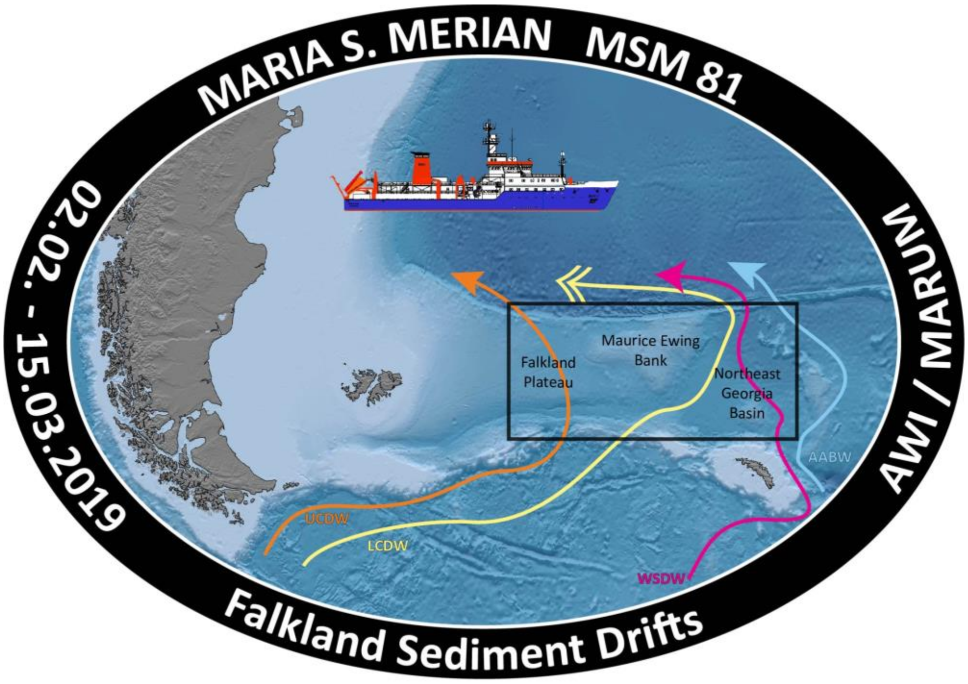

Dr. Gabriele Uenzelmann-Neben

Alfred-Wegener-Institut Helmholtz-Zentrum für Polar- und Meeresforschung

2019

Table of Contents

1 Cruise Summary

1.1 Summary in English

Cruise Leg MSM81 with RV *MARIA S. MERIAN*, leaving Valparaiso, Chile, on February 2 2019, returning to Montevideo, Uruguay, on March 15 2019, comprised seismic reflection studies of the Falkland Plateau, the westernmost part of the Agulhas-Falkland Fracture Zone in the South Atlantic. The Falkland Plateau rises up 1500 m above the surrounding seafloor and hence forms an obstacle for the exchange of water masses between high and lower latitudes. A water mass exchange between the Pacific and Atlantic oceans has been enabled with the opening of Drake Passage. In this way heat and energy could be transferred between the two oceans. A detailed study and analysis of the structure of the Falkland Plateau and channel in the south via seismic data and a correlation with results from DSDP Leg 36 Sites 327, 329, and 330 as well as Leg 71 Site 511 was needed to supply information on the Cretaceous and Tertiary development of the Falkland Plateau and its influence on the path of the Antarctic Circumpolar Current, Upper and Lower Circumpolar Deepwater, South Pacific Deepwater, and Weddell Sea Deepwater. Seismic profiles were gathered, which capture the structure of the Falkland Plateau to basement and possible sediment drifts. In total ~5200 km of high resolution seismic reflection data were recorded. Bathymetric and Parasound data were recorded parallel to the seismic profiling.

To complement the seismic studies SVP and XSV measurements at six locations and ADCP measurements across the whole working area were carried out.

1.2 Zusammenfassung

Der Fahrtabschnitt MSM81 vom 2. Februar 2019 Valparaiso, Chile, bis 15. März 2019 Montevideo, Uruguay, mit FS *MARIA S. MERIAN* bestand aus reflexionsseismischen Untersuchungen des Falkland Plateaus, der westlichen Struktur in der Agulhas-Falkland Fracture Zone im Südatlantik. Das Falkland Plateau erhebt sich bis auf 1500 m Wassertief und formt so eine Barriere für den Austausch von Wassermassen zwischen hohen und mittleren Breiten. Ein Wassermassenaustausch zwischen Pazifik und Atlantik wurde durch die Öffnung der Drake Passage ermöglicht. Auf diese Weise kam es auch zum Austausch von Energie und Wärme. Eine detaillierte Erfassung und Analyse der Struktur des Falkland Plateaus und der südlich gelegenen Rinne mittels seismischer Methoden und ein Anschluß an bestehende DSDP Bohrungen (DSDP Legs 36 und 71) wurde benötigt, um Informationen über die spätkretazische und tertiäre Entwicklung des Falkland Plateaus und seinen Einfluß auf die Entwicklung der Pfade des Antarktischen Zirkumpolarstroms, des Oberen und Unteren Zirkumpolaren Tiefenwassers, des Pazifischen Tiefenwassers und des Weddell Tiefenwassers zu erhalten. Das reflexionsseismische Programm während der Expedition MSM81wurde derart gestaltet, dass die Struktur des Falkland Plateaus bis zum Basement sowie mögliche Sedimentdrifts erfasst wurden. Es wurden insgesamt ~5200 km an hochauflösenden reflexionsseismischen Daten registriert. Parallel zu den seismischen Profilarbeiten wurden bathymetrische und Parasound Messungen durchgeführt.

Ergänzt wurden die seismischen Messungen durch sechs SVP und XSV Stationen und ADCP Messungen im Gebiet des Falkland Plateaus.

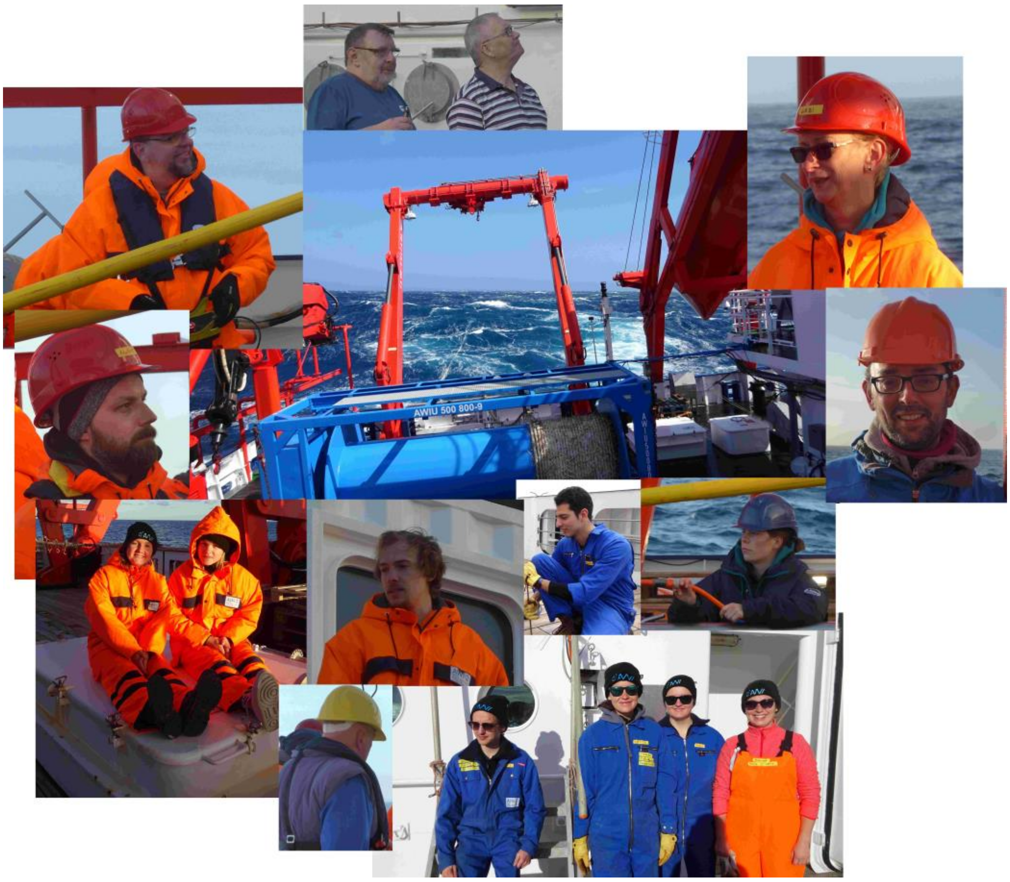

Fig. 1.1 Scientific team of cruise MSM81.

2 Participants

2.1 Principal Investigators

Name	Institution
Uenzelmann-Neben, Gabriele, Dr.	AWI
Westerhold, Thomas, Dr.	MARUM

2.2 Scientific Party

Name	Discipline	Institution
Uenzelmann-Neben, Gabriele	Marine Seismics / Chief Scientist	AWI
Eggers, Thorsten	Marine Seismics	AWI
Lensch, Norbert	Marine Seismics	AWI
Pfeiffer, Adalbert	Marine Seismics	AWI
Beckmann, Regina	Marine Seismics	AWI
Nüsse, Amelie	Marine Seismics	AWI
Andreas, Pascal	Marine Seismics	AWI
Petersen, Ann-Kathrin	Marine Seismics	AWI
Geils, Jonah	Bathymetry	AWI
Knopp, Lisa	Bathymetry	AWI
Andree, Sophie	Bathymetry	AWI
Westerhold, Thomas	Parasound	MARUM
Ramadan, Abdel-Rahman	Parasound	AWI
Reuter, Runa	Parasound	AWI
Gatt, Peter	Marine Mammal Observer	SFF
Soutar, George	Marine Mammal Observer	SFF
Mouchel-Drillot, Mathieu	Marine Seismics	SERCEL
Neuilly, Alexandre	Marine Seismics	SERCEL
Principi, Sebastian	Observer Coastal State Argentina	IGEBA

2.3 Participating Institutions

AWI	Alfred-Wegener-Institut Helmholtz-Zentrum für Polar- und Meeresforschung Bremerhaven
IGEBA	Buenos Aires' Basic Geoscience Institute
MARUM	Zentrum für Marine Umweltwissenschaften Bremen
SFF	SFF Services Limited
SERCEL	Sercel France

2.4 Crew

Name	Rank
Schmidt, Ralf	Kapitän / Master
Peters, Ralf	Ltd Offizier/ Chief Officer
Janssen, Sören	1. Offizier/ 1st Officer
Kruse, Marius	2. Offizier/ 2nd Officer
Angelis, Wilhelm	2. Offizier/ 2nd Officer
Ogrodnik, Thomas	Ltd Ingenieur/Chief Engineer
Boy, Manfred	2. Ingenieur/ 2nd Engineer
Schwieger, Philipp	3. Ingenieur/ 3rd Engineer
Maggiulli, Michael	System Operator
Walter, Jörg	Eletroniker/ Electronics
Hermann, Jens	Elektriker/ Electrics
Wiechert, Olaf	Deckschlosser/ Fitter
Meyer, Felix	Motormann/ Oiler
Bosselmann, Norbert	Bootsmann/ Bosun
Wolff, Andreas	Schiffsmechaniker, SM
Vredenborg, Enno	Schiffsmechaniker, SM
Schrapel, Andreas	Schiffsmechaniker, SM
Peschel, Jens	Schiffsmechaniker, SM
Werner, André	Schiffsmechaniker, SM
Plink, Sebastian	Schiffsmechaniker, SM
Siefken, Tobias	Schiffsmechaniker, SM
Matter, Sebastian	1. Koch/ 1st Cook
Streifling, Stefan	2. Koch/2nd Cook
Seidel, Iris	Stewardess
Staak, Ludwig	Bordarzt/ Ship's Doctor

3 Research Program

(G. Uenzelmann-Neben[1], T. Westerhold[2])
[1]AWI
[2]MARUM

3.1 Aims of the Cruise

The South American gateway comprising Drake Passage and the Scotia Sea is of huge importance because its opening enabled the exchange of deep water masses and energy between the southern Pacific and the South Atlantic. This in combination with opening of the Tasman Gateway enabled the establishment of the clockwise flowing Antarctic Circumpolar Current (ACC) at the Eocene/Oligocene boundary. The onset of the ACC caused the thermal isolation of the Antarctic continent which has been considered as a prerequisite for the onset of widespread glaciation in Antarctica by some researchers (e.g., Barker and Thomas, 2004; Livermore *et al.*, 2007; Zachos *et* *al.*, 2001), whereas other authors favour a major drop in atmospheric CO_2 concentrations as the main trigger for Antarctic glaciation (e.g., Coxall *et al.*, 2005; DeConto *et al.*, 2008; Pagani *et al.*, 2005). Recently, a coupled ocean-atmosphere model based study (Goldner *et al.*, 2014) proposed a major reorganisation of the ocean circulation by the Antarctic glaciation at the Eocene/Oligocene boundary strengthening Antarctic Intermediate Water flow to the north as well as invigorating the formation of Antarctic Bottom Water.

The overaching goals of the cruise MSM81 Falkland Sediment Drifts were twofold: we intended to 1) study variations in flow paths and intensities of deep and bottom water masses in response to a) tectonic movements, and b) climate variability; this has been the major focus of the cruise, and 2) collect pre-site survey data for IODP proposal 862-Pre.

Objective 1: Reconstruct variations in flow path and intensities of deep and bottom water masses

The deep and bottom water masses flowing within the ACC (Antarctic Bottom Water (AABW), WSDW, SPDW, LCDW, UCDW) are steered by the complex topography of the Drake Passage and the Scotia Sea (Figs. 3.1 and 3.2). Rounding topographic highs the water masses reduce their speed and hence deposit sediment. In gaps and passages their speed is increased leading to erosion and non-deposition. In this way the aforementioned water masses shape sediment drifts, which in their structure (geometry, internal unconformities, reflection characteristics) document the modifications in the flow paths and intensities of the water masses. The tectonic development of both the Drake Passage and the Scotia Sea during the Cenozoic have led to strong modifications in the flow paths, which, when studying sediment drifts, can be deciphered. Additionally, the ACC fronts are assumed to have been subject to relocations during glacial-interglacial cycles. This again has led to relocations in depocentres, which can be identified via seismic profiles. So far, research here has concentrated on the area south of the Falkland Islands towards South America (Koenitz *et al.*, 2008; Pérez *et al.*, 2015) but the flow of water masses across the plateau has not been studied. Results of DSDP Legs 36 and 71 suggested intensified bottom currents as early as the Eocene, which led to the discussion of an early Tertiary water mass exchange between the Pacific and the Atlantic oceans (Shipboard_Scientific_Party, 1977, 1980). Numerical simulations also suggest a weak ACC for the late Cretaceous but no overturning circulation (Uenzelmann-Neben *et al.*, 2017).

The questions we intended to answer have been the following:

- When and how did the onset of the ACC and the deep and bottom water masses flowing within the ACC affect sedimentation at the Falkland Plateau area?
- When can we recognise the first overspill of UCDW and LCDW over the Falkland Plateau indicating transport of cold water masses into the South Atlantic?
- What are the variations of the pathways and intensity of overspill and the location of the ACC fronts in relation to a) tectonic movements, and b) modifications in climate (e.g. Mid-Miocene Climatic Optimum and Transition, Pliocene warming, onset of widespread glaciation on the Northern Hemisphere)?

To answer those questions we collected a set of high-resolution (1 ms sample rate, 500 Hz max frequency, 80 Hz dominant frequency≅ 9 m vertical resolution, 240 channels, 25 m shot interval) seismic profiles on the Falkland Ridge between a) the Falkland Islands and the MEB (Fig. 5.3).

This set of seismic lines will enable the detection and imaging of sediment drifts shaped by UCDW west of MEB and shaped by LCDW and WSDW in the channel south of the plateau and MEB (Fig. 3.1). The seismic lines further crossed the locations of DSDP Leg 36 Sites 327 and 329 and Leg 71 Sites 511 and 512. Those sites recovered sedimentary rocks going back towards the Jurassic (Site 511, Ciesielski and Weaver, 1980), were used for dating regional seismic reflections (Ciesielski and Weaver, 1980; Shipboard_Scientific_Party, 1977), and, via the computation of synthetic seismograms, will thus allow to correlate the acquired seismic data with geological information (lithology, sediment composition, grain sizes, etc) and to develop age-depth models. The new seismic profiles hence will provide information on the depositional regime (location/relocation and orientation of depocentres, sedimentary structures, e.g., sediment drifts and waves, erosional structures) prior, during, and following the opening of Drake Passage by imaging the sedimentary sequences and structures for those periods. We will be able to reconstruct the effect of the onset of the ACC on sediment deposition and the modifications in ACC pathway and flow intensity due to tectonic movements and climate variability. Sediment drifts located in the Falkland Passage east of MEB are particularly important targets because they should be sensitive recorders of past relocations of the SACCF retroflection and of past changes in both WSDW and LCDW flow (Naveira Garabato *et al.*, 2002; Sokolov and Rintoul, 2009).

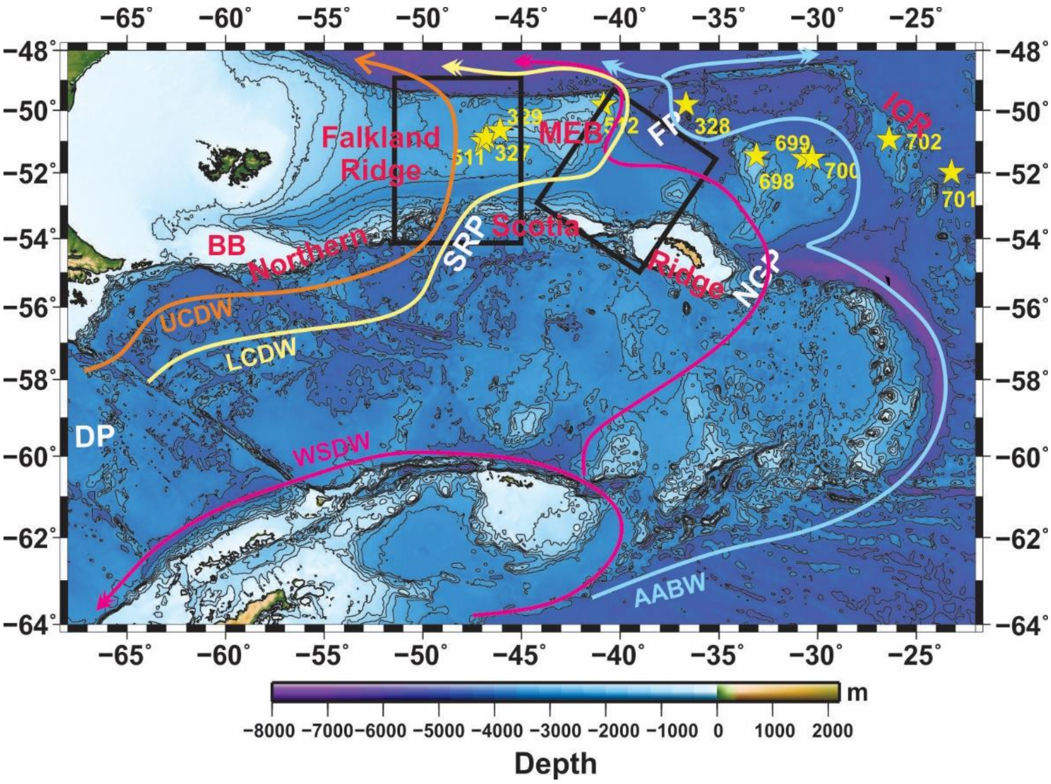

Fig. 3.1 Bathymetric map of the Drake Passage (DP), the Scotia Sea, and the Falkland Plateau (Smith and Sandwell, 1997). The arrows schematically show the present pathways of Upper Circumpolar Deepwater (UCDW), Lower Circumpolar Deepwater (LCDW), Weddell Sea Deep Water (WSDW), and Antarctic Bottomwater (AABW). The yellow stars show the locations of DSDP Leg 36 Sites 327, 238, and 329 and Leg 71 Sites 511 and 512 as well as ODP Leg 114 Sites 698, 699, 700, 701, and 701 (Ciesielski and Weaver, 1980; Shipboard_Scientific_Party, 1977, 1988). BB= Burdwood Bank, FP= Falkland Passage, IOR= Islas Orcadas Rise, MEB= Maurice Ewing Bank, NGP= North Georgia Passage, SRP= Shag Rock Passage.

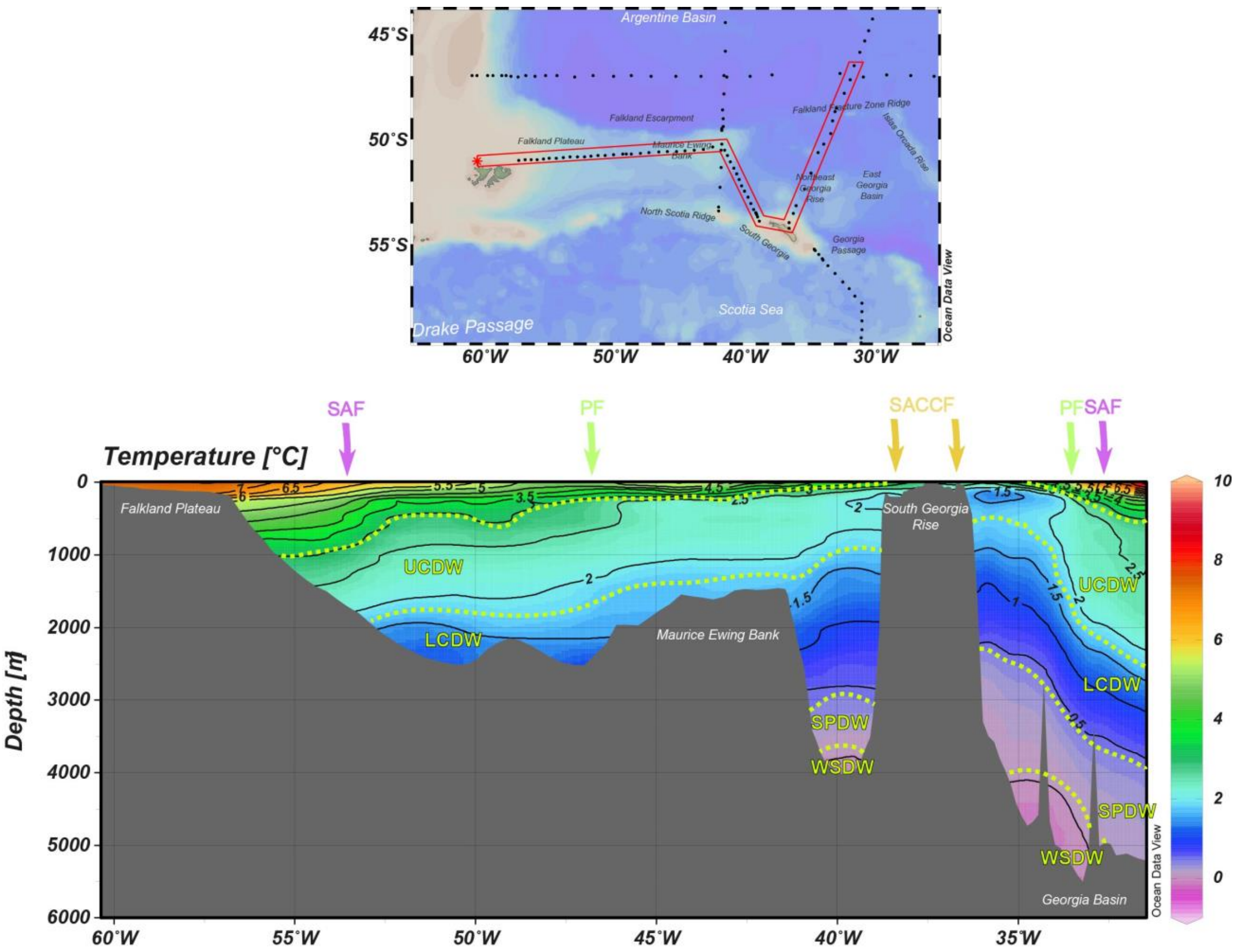

Fig. 3.2 Temperature profile across the Falkland Plateau showing the different water masses, LCDW= Lower Circumpolar Deepwater, UCDW= Upper Circumpolar Deepwater, SPDW= Southern Pacific Deepwater, WSDW= Weddell Sea Deepwater. PF= Polarfront, SACCF= Southern ACC Front, SAF= Subantarctic Front. Generated using Ocean data View (Schlitzer, 2013).

Objective 2: Pre-site survey for developing a full IODP proposal built on IODP 862-Pre

IODP preliminary proposal 862-Pre (PIs Westerhold and Bohaty) proposes to drill a depth transect of Paleogene sites in the subantarctic South Atlantic Ocean on the eastern Falkland Plateau (Maurice Ewing Bank and Georgia Basin). In the modern ocean, this is a critical area for deep-water mixing and communication between the Pacific and Atlantic oceans across the Drake Passage, with local bathymetry controlling the dispersal and propagation of deep- and bottom-waters throughout the Atlantic. Proposal 862-Pre intends to recover a composite of Paleogene sections spanning an extensive range of palaeo-water depths (~500-4500 m). The primary focus will be on determining the timing and variability of shallow- and deep-water connectivity across the Drake Passage and testing whether the onset of a proto-Antarctic Circumpolar Current (ACC) circulation had a direct impact on high-latitude and global climate evolution. The drill cores will provide crucial insight on the long-standing question of the relative influence of atmospheric pCO_2 drawdown vs. Southern Ocean gateways in driving Paleogene climate evolution. The target sites will be positioned to assess the relationships between local tectonic subsidence of deep-water barriers, high-latitude climate change, and the onset of bottom-water production in the Weddell Sea and northward propagation into to the deep western Atlantic. This development along with the onset of the ACC circulation fundamentally altered Cenozoic ocean circulation in the Atlantic.

This way new light will be shed on climate change, biotic shifts, and deep-sea chemistry during the Paleogene, allowing evaluation of: (i) the magnitude of temperature change and response of high-latitude plankton groups across transient 'greenhouse' events, (ii) the initiation of southern high latitude cooling and onset of Antarctic Peninsula glaciation during the middle Eocene–early Oligocene 'greenhouse' to 'icehouse' transition, and (iii) variation in the Calcite Compensation Depth in the South Atlantic and its relation to changes in global carbon cycling.

One of the challenging elements of high latitude Southern Ocean palaeoceanography is site selection. In order to choose sites, where a sedimentary column appropriate to achieve the goals of a full IODP proposal can be drilled, high-resolution seismic data were needed. Based on the new seismic data collected during cruise MSM81 primary drill sites and several alternate sites have to be determined, which will be important if there is poor recovery due to chert or other drilling challenges. We collected a set of seismic profiles, which have covered the locations of piston cores collected druing cruise DY087 with HMS *Discovery* in 2018 (chief scientist Dr. S Bohaty, Southampton).

3.2 Agenda of the Cruise

The main objective of cruise MSM81 was the collection of high resolution seismic reflection data to identify sedimentary structures shaped by deep and bottom water masses. To prepare for the cruise an environmental impact assessment was carried out by BMT UK 2 Ltd. This EIA comprised an evaluation of all noise sources during the cruise: the seismic sources, the vessel itself, Parasound, and the multibeam system EM 122. Noise predictions have been undertaken for the proposed geophysical survey between Falkland Islands and South Georgia waters and applied to the latest published international thresholds (NMFS, 2016 and 2018a). The results indicated that none of the applicable injury thresholds would be breached outwith approximately 150 m from the operation. Animals may be within around 800 m of the source. A mitigation zone of 500 m was found to be appropriate to control the risks from underwater noise. The JNCC protocol has been designed to apply to distances of this magnitude in order to reduce the risk of injury to marine mammals to negligible levels. Furthermore, below mitigation measure were suggested:

- Deploying a marine mammal observer;
- Maintain a 500 m mitigation zone;
- Avoiding starting piling at night or in poor visibility (unless further mitigation such as PAM is provided);
- Searching for animals in the mitigation zone for a minimum of 60 minutes before starting, to allow for deep-diving species to surface;
- Waiting for 20 minutes after the last observation of mammals in the mitigation zone;
- Apply a 20-minute soft start to the seismic airgun, e.g., by increasing from one gun up to four;
- Repeat the process if there is a break of over 10 minutes;
- If line changes are expected to take longer than 40 minutes, firing is to be terminated at the end of the survey line and the mitigation process repeated; and
- Report the activity and any observations using the standard format.

Additionally, applications for an environmental permit were handed in to the authorities of the Falkland Islands and South Georgia. Those permits were issued.

We hired two independent Marine Mammal Observers from SFF to watch out for marine mammals prior and during seismic profiling. Their report will be filed after completion of the cruise. Our streamer system has also included a Passive Acoustic Monitoring (PAM) system, Quiet Sea™ by Sercel. This supported the MMOs and allowed line changes during night.

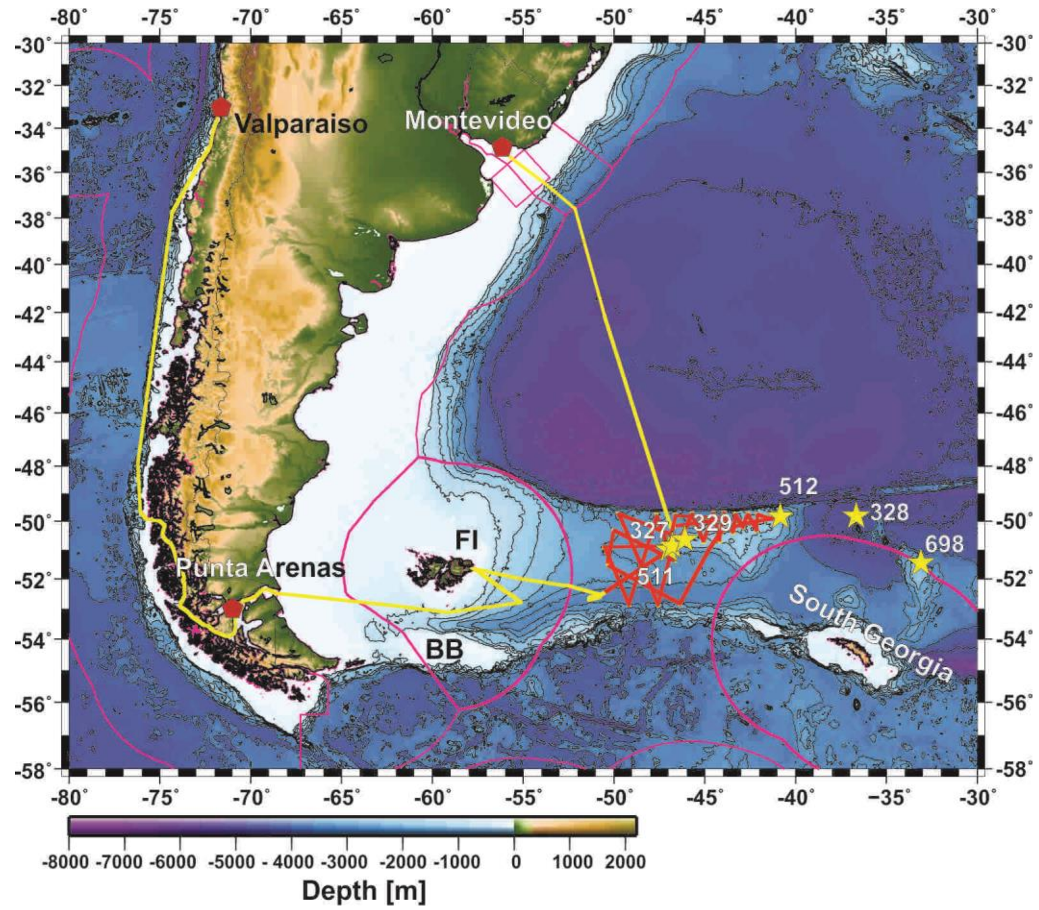

Fig. 3.1 Track chart (yellow lines) of cruise MSM81. Bathymetry from Smith and Sandwell (1997). Red lines show the seismic profiles collected on the Falkland Plateau. Pink lines show the boundaries of the EEZs.

4 Narrative of the Cruise

(G. Uenzelmann-Neben[1])
[1]AWI

The final preparations for cruise MSM were carried out on board RV *MARIA S MERIAN*. 18 Scientists embarked in Valparaiso on February 2 and unloaded containers. The set-up of the seismic sources and the recording system began. RV *MARIA S MERIAN* left port on February 3 at appr. 18:40 to head south. Set-up of the seismic equipment continued during February 4 to 8. On February 8 RV *MARIA S MERIAN* arrived in Punta Arenas to bunker. Here, two technicians from Sercel, who had assisted in installing new parts of the seismic recording system, left, while an Argentine coastal state observer was welcomed on board. The vessel left the port on February 9 at 9:00 to head into the working area on the Falkland Plateau. During this transit preparations for the seismic sources to be used during MSM82 started.

RV *MARIA S MERIAN* entered Argentine waters on February 9 at 18:30, and the recording of EM 122 and Parasound started. The transit into working area continued, entering the Argentine EEZ and entering the EEZ of the Falkland Islands on February 10 at 9:55, but was interrupted on February 11 due to the emergency disembarkment of one person. We then set course for Port Stanley, Falkland Island to allow the crewman to fly home. After the crewman disembarked on late evening February 11 we continued our transit into the working area. We left the EEZ of the Falkland Islands on February 12 at 16:27.

At 22:00 February 12 we reached our area of investigation. We then obtained a sound velocity profile to calibrate both EM 122 and Parasound. Since the weather had severely deteriorated, we had 9 bft and 6 m waves, we postponed the deployment of the seismic gear to the next morning. The wind still was very strong (8-9 bft) but the waves only reached 5 m and deployment was easier in daylight. We continuously collected seismic data. Repairs were carried out on February 21st, March 2nd, and March 6th, which generated short losses in data acquisition. Since we did not stop we could not collect additional sound velocity profiles using the SVP device but employed XSVs instead, which can be used during seismic profiling.

At 16:00 on March 10 we reached the end of line AWI-20190030 and stopped the collection of seismic and Parasound data. We retrieved airguns and streamer and set course for Montevideo. We stopped the bathymetric recordings at 22:00 on March 13th. We arrived in Montevideo on March 15 2019 at 8:30.

5 Preliminary Results

5.1 Seismic Reflection Profiling

(G. Uenzelmann-Neben[1], P. Andreas[1], R. Beckmann[1], T. Eggers[1], N. Lensch[1], A. Nüsse[1], A.K. Petersen[1], A. Pfeiffer[1])

[1]AWI

The application of seismic methods was one of the primary operational objectives of MSM81 in order to obtain information on the structure and sedimentary distribution in the area of the Falkland Plateau. We used a standard multi-channel seismic reflection technique to image the outline and reflectivity characteristics of the sedimentary layers and the structure of the sub-sedimentary basement and lower crust by recording the returning near-vertical wave field. Figure 5.1 illustrates the principles of this technique.

5.1.1 Seismic Equipment

(T. Eggers[1])

[1]AWI

5.1.1.1 Seismic Sources, Activation and Timing

We used a cluster of 4 GI-guns to resolve the sedimentary layers. A single GI-Gun is made up of two independent air guns within the same body. The first air gun (“Generator”) produces the primary pulse, while the second air gun (“Injector”) is used to control the oscillation of the bubble produced by the “Generator”. We used the “Generator” with a volume of 0.72 liters (45 in^3) and fired the “Injector” (1.68 liters = 105 in^3) with a delay of 33 ms. This leads to an almost bubble-free signal. The guns were towed 20 m behind the vessel in 2 m depth and fired every 25 m (□20 s shot interval).

The activation of the airguns occurs through a gun controller (Teledyne BigShot™). The controller provides the power necessary to activate the valves of the guns. With an optional feedback signal from extra hydrophones, the controller is capable of synchronizing the activation of each gun automatically. This ensures that the complete gun array fires at the same time. The gun controller itself waits for the fire order (TTL signal) of the navigation system.

Seismic data acquisition requires a very precise timing system, because seismic sources and recordings systems must be synchronised. All the systems are synchronised through a dedicated GPS clock with an accuracy of 1µs.

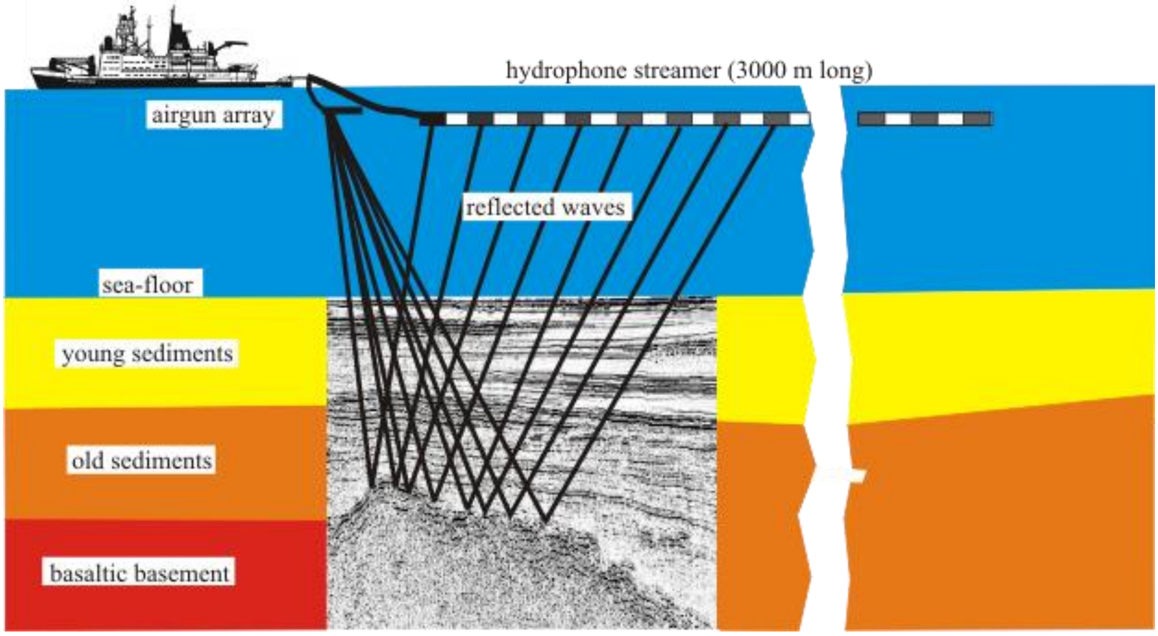

Fig. 5.1 Principle of marine seismic reflection surveying.

5.1.1.2 Navigation and Triggering

For planning the lines and performing the line shooting, we are using a separate navigation system (Sercel SeaPro Nav™). From ship side, we get NMEA strings for the ship position, heading, water depth and speed through water. Depending on the actual plan, the navigation system calculates the next shot point as defined by the shot parameters (shot distance, time or a combination of both) and generates the fire order for the air guns. After each successfully performed shot, the navigation system generates a navigation header file and transfers it to the acquisition system. This file uses the SEAL™ acquisition system to generate the final SEGD file for this shot point.

5.1.1.3 Multi-Channel Reflection Recording System

For multi-channel reflection data acquisition, a complete digital seismic streamer and recording system was used. The system consists of a large capacity, fully integrated, high resolution marine seismic data acquisition system (Sercel SEAL□) (Fig. 5.2). The streamer is a 240-channel hydrophone array, composed of 20 active sections with 12 channels each. Each channels consists of 8 hydrophones placed in an array. The spacing of each hydrophone array is 12.5 m (Table 5.1).

The streamer is coupled to the on-board recording system via a fiber-optic tow leader and a deck lead. The data collected by the hydrophone array is firstly converted from an analogue signal to digital via a Field Digitizing Unit (FDU2F). The data is available as a 24-Bit word with a sample rate of 1, 2 or 4 ms and then routed through a Line Acquisition Unit Marine (LAUM). After filtering and compressing the data, the LAUM sends them to the on-board equipment. The LAUM also supplies power for the FDU2F, and they are located after every 5 active sections.

The interface to the on-board equipment is the Deck Cable Crossing Unit (DCXU). It has a build-in high-voltage power supply for powering all the streamer modules and acts as a LAUM for first 60 channels.

The main software is installed on a server running Linux Operating System mounted with the other components in a mobile rack. It manages the flow of acquired data from the streamer and auxiliary channels. It also manages processing of the data and export to various peripherals (FC-AL tape drives, NFS disks, plotters, QC tools). Communications and synchronization with the navigation system are ensured via Ethernet links or a T0 signal. Communications with DCXU-428s are ensured via Ethernet links too, therefore the server can manage a virtually unlimited number of DCXU-428s (streamers). The system and all parameters for acquisition are displayed and controlled on a separate client pc with a graphical user interface (GUI).

The acquisition runs in continuous mode and the final SEGD file for a shot point will be generated according to the navigation header file, received from the navigation system. The final SEGD file is stored on the server and exported simultaneously to two Network Attached Storage (NAS) with a capacity of 5 TB each. The actual SEGD for the last shot point is also available for the QC-Software running on a separate client. With this software, it is possible to have a first look on the data for quality control.

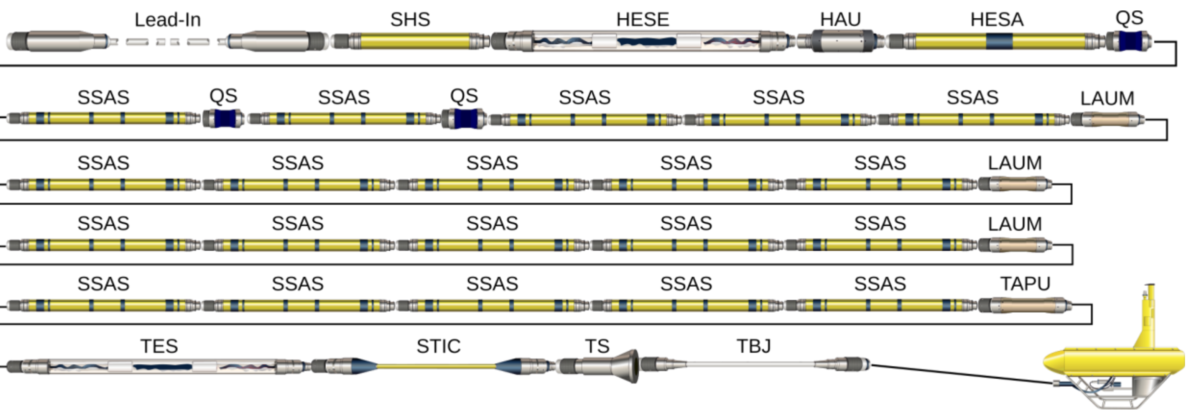

Fig. 5.2 Setup of the seismic data acquisition.

5.1.1.4 Depth Control and Positioning

With depth control units, called birds, we can control the depth of the streamer cable during operation. We use Model 5010/5011 DigiBIRD™ and CompassBIRD™ II from ION, controlled by Digicourse™ software, for this purpose. Nominal depth of the streamer cable in calm weather conditions is 10m. The depth can be changed during operation by setting new target depths for each bird through the controller software.The actual depth and heading (only Model 5011 DigiBIRD™ and CompassBIRD™ II) of each bird is available for the navigation system and will be stored for every shotpoint.

5.1.1.5 Passive Acoustic Monitoring

We use QuietSea™ from Sercel for passive acoustic monitoring. The system can detect vocalizations emitted by marine mammals. These signals are of two types: whistles and click trains. The whistles are particular vocalizations emitted to communicate between marine mammals in the same group or are parts of a song call emitted by specific baleen whale males.

The clicks are impulsive signals (from approximately ten microseconds to few milliseconds) and so cover a great bandwidth. The bandwidth covered by clicks can be highly variable depending on the species.

The system uses the seismic data (using the SEAL□ interface) to detect vocalizations in the seismic bandwidth (from 10 Hz to 200 Hz with usual seismic sampling frequency of 2ms). It also uses dedicated streamer modules and auxiliary modules to detect localizations in the [200 Hz-96 kHz] bandwidth.

Table 5.1 Specification of SENTINEL**™** active section, 12.5m spacing

Field Digitizing Units (FDUs).	
Arrangement	One per receiver point (2 channels)
Functions	A/D conversion, data digitizing, and tests
FDUs per active section	6 (2 per location)
Spacing	50m
Hydrophones	
Standard model	Sercel Flexible Hydrophone (SFH)
Nominal capacitance	32.5 nF ± 10% @ 20º C
Nominal sensitivity	–192.9 dB ref to 1 V/µPa ± 1.5 dB (22.65 V/bar) @ 20º C
Hydrophone Array	
Cut off frequency	2 Hz
Groups per section	12
Hydrophones per group	8
Group capacitance (nominal)	260 nF ± 10% @ 20° C
Group sensitivity	–194.1 dB ref to 1 V/µPa ± 1.0 dB (19.7 V/bar) @20° C

The data were recorded with the following parameters (also Appendix B):

Table 5.2 Brief description of seismic recording parameters.

Profile Name	*Active Length*	*Lead-in*	*Record Length*	*Sample Rate*
AWI-20190001	3000 m	141.4 m	9 s	1 ms
AWI-20190002	3000 m	141.4 m	9 s	1 ms
AWI-20190003	3000 m	141.4 m	9 s	1 ms
AWI-20190004	3000 m	141.4 m	9 s	1 ms
AWI-20190005	3000 m	141.4 m	9 s	1 ms

AWI-20190006	3000 m	141.4 m	9 s	1 ms
AWI-20190007	3000 m	141.4 m	9 s	1 ms
AWI-20190008	3000 m	141.4 m	9 s	1 ms
AWI-20190009	3000 m	141.4 m	9 s	1 ms
AWI-20190010	3000 m	141.4 m	9 s	1 ms
AWI-20190011	3000 m	141.4 m	9 s	1 ms
AWI-20190012	3000 m	141.4 m	9 s	1 ms
AWI-20190013	3000 m	141.4 m	9 s	1 ms
AWI-20190014	3000 m	141.4 m	9 s	1 ms
AWI-20190015	3000 m	141.4 m	9 s	1 ms
AWI-20190016	3000 m	141.4 m	9 s	1 ms
AWI-20190017	3000 m	141.4 m	9 s	1 ms
AWI-20190018	3000 m	141.4 m	9 s	1 ms
AWI-20190019	3000 m	141.4 m	9 s	1 ms
AWI-20190020	3000 m	141.4 m	9 s	1 ms
AWI-20190021	3000 m	141.4 m	9 s	1 ms
AWI-20190022	3000 m	141.4 m	9 s	1 ms
AWI-20190023	3000 m	141.4 m	9 s	1 ms
AWI-20190024	3000 m	141.4 m	9 s	1 ms
AWI-20190025	3000 m	141.4 m	9 s	1 ms
AWI-20190026	3000 m	141.4 m	9 s	1 ms
AWI-20190027	3000 m	141.4 m	9 s	1 ms
AWI-20190028	3000 m	141.4 m	9 s	1 ms
AWI-20190029	3000 m	141.4 m	9 s	1 ms
AWI-20190030	3000 m	141.4 m	9 s	1 ms

5.1.1.6 First Results

(G. Uenzelmann-Neben[1])

[1]AWI

The seismic grid was set up to image the structure of both basement and sedimentary rocks on the Falkland Plateau as well as the channel south of the plateau. Because of the size of the Falkland Plateau and the published pathways of Upper and Lower Circumpolar Deepwater (UCDW, LCDW) we concentrated our seismic profiling on the western flank of the Maurice Ewing Bank, which forms a high on the eastern plateau, and the slight depression west of it. This allowed a direct correlation with results from DSDP Leg 36 Sites 327, 329, and 330 and DSDP Leg 71 Site 511 (Fig. 5.3). Additionally, we covered the locations of several potential site for IODP proposal 862, where gravity cores were during expedition DY087 with HMS *Discovery* (Chief Scientist Dr. S. Bohaty, Southampton). In total, 30 seismic profiles were gathered across the Falkland Plateau (Fig. 5.3).

About 2 Tb of raw data were gathered. Due to this large amount the data were only converted into the internal format of our processing system Echos™, the shot-CDP geometry was defined, and the data were sorted. Afterwards, constant offset plots were created for quality control. The remaining processing steps will be carried by a PhD student. A proposal for funds has been submitted to the DFG priority programme IODP.

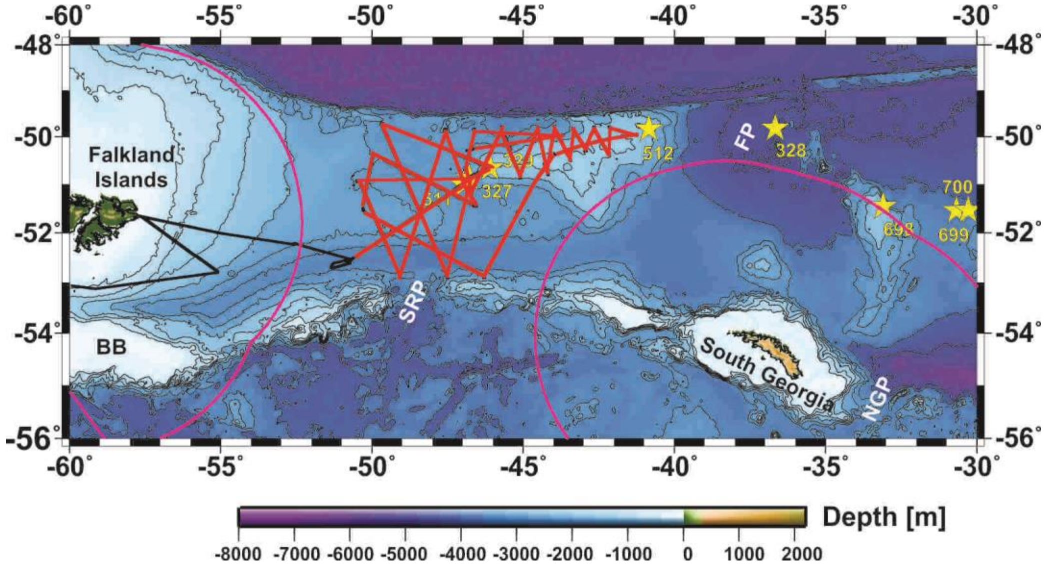

Fig. 5.3 Bathymetric map of the Falkland Plateau showing the locations of the collected seismic profiles (red lines) and of DSDP Leg 36 Site, 327, 328, 329, and 330, and Leg 71 Site 511 and 512 (yellow stars). Also shown are the locations of ODP Leg 114 Sites 698, 699, and 700. The magenta lines show the boundaries of the Falkland Islands' EEZ and the EEZ of South Georgia. BB= Burdwood Bank, FP= Falkland Passage, NGP= North Georgia Gap, SRP= Shag Rock Passage.

The seismic data are of excellent quality. Although using only small sources (four GI-guns with a total volume of 9.6 l) the seismic signals have penetrated up to 3 s TWT (~3 km) of the sedimentary column. With our first seismic profile we crossed all four sites drilled on the western MEB (Figs. 5.3 and 5.4). We also crossed Site 511 with lines AWI-20190008, Site 327 with lines AWI-2019004 and -20190005, and Site 329 with line AWI-20190002. This enabled a first tentative correlation of observed seismic reflections with ages derived at the drill sites. In general, the seismic data across the whole of the plateau show a number of distinct horizons and erosional unconformities, e.g., the Eocene/Oligocene boundary, the top Maastrichtian, the Albian/Aptian boundary (Fig. 5.4). The top of the Precambrian basement also is imaged very well. Additionally, several prominent reflections between the Cenomanian and Maastrichtian horizons can be observed (Fig. 5.5).

The central Falkland Plateau appears to be underlain by a number of Precambrian highs, which are imaged up to the Maastrichtian reflection (Fig. 5.5). Those basement highs sometimes are wide but in some cases appear quite narrow, e.g., towards to the Maurice Ewing Bank (see Fig. 5.5). Those narrow basement highs may point towards a tectono-magmatic reactivation of the plateau. The southern flank of the plateau is characterised by an outer high imaged up to the Albian/Aptian. The Maastrichtian sequences also are characterised by local highs (e.g., Fig. 5.4). Those sometimes are cone-shaped, and can be found on the Falkland Plateau and the MEB (Fig. 5.5, see near location of DSDP Site 327).

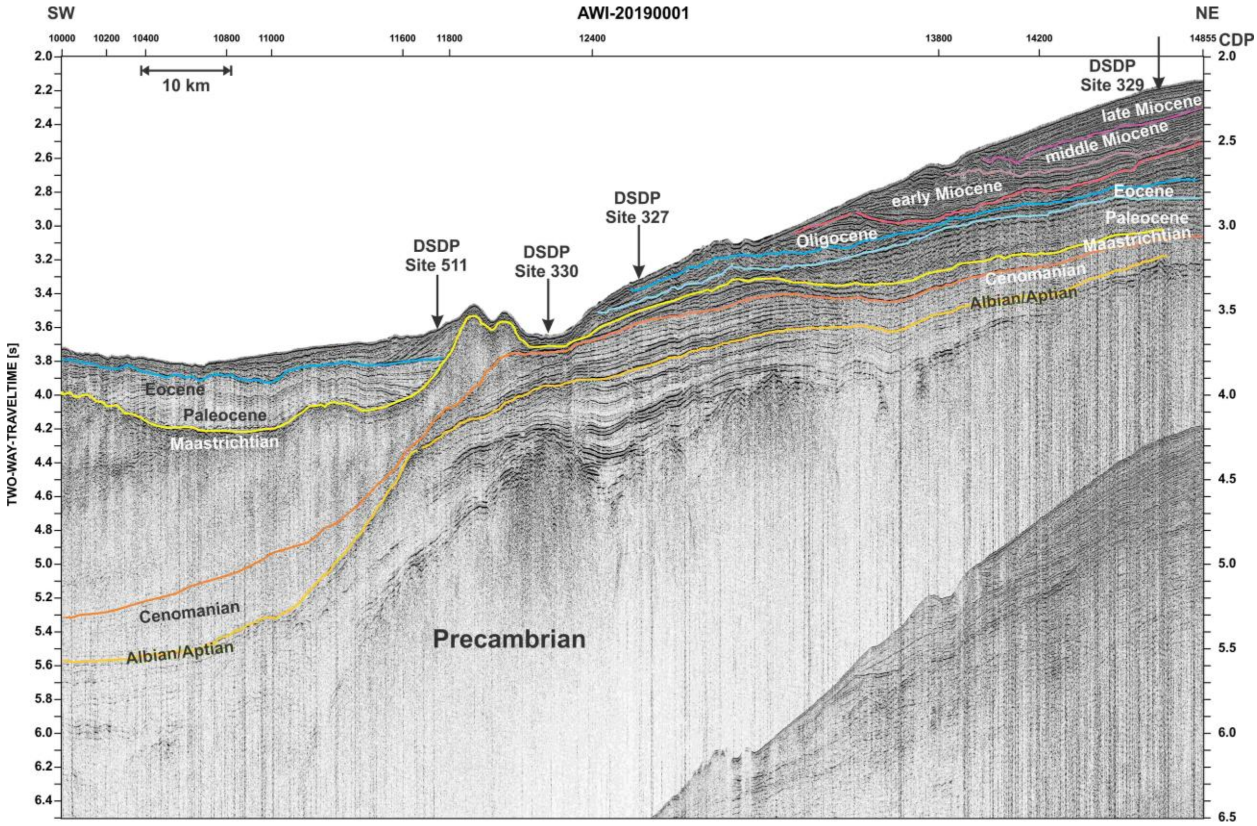

Fig. 5.4 Part of seismic reflection profile AWI-20190001 showing the locations of DSDP Leg 36 Site, 327, 329, and 330, and Leg 71 Site 511. A tentative correlation with ages derived at the drill sites allowed a first dating of the reflections.

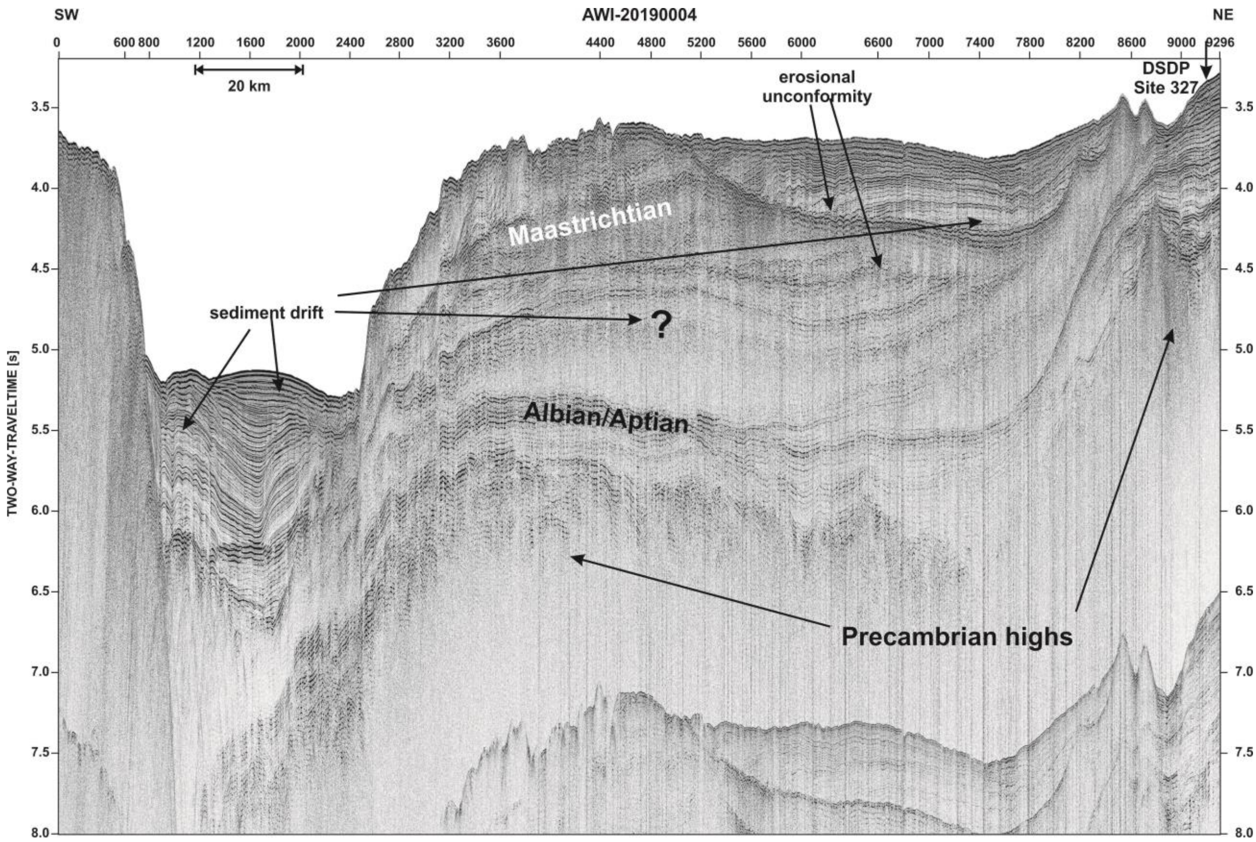

Fig. 5.5 Seismic reflection profile AWI-20190004 across the Falkland Plateau. Note the channel in the South. Site 327 was crossed in the North.

The sequence between the Cenomanian and the Maastrichtian reflections is characterised by a thick sediment wedge. At a first glance this may be interpreted as a sediment drift, which would indicate overflow activity already in late Cretaceous times. Further careful analysis is needed after the data have been fully processed.

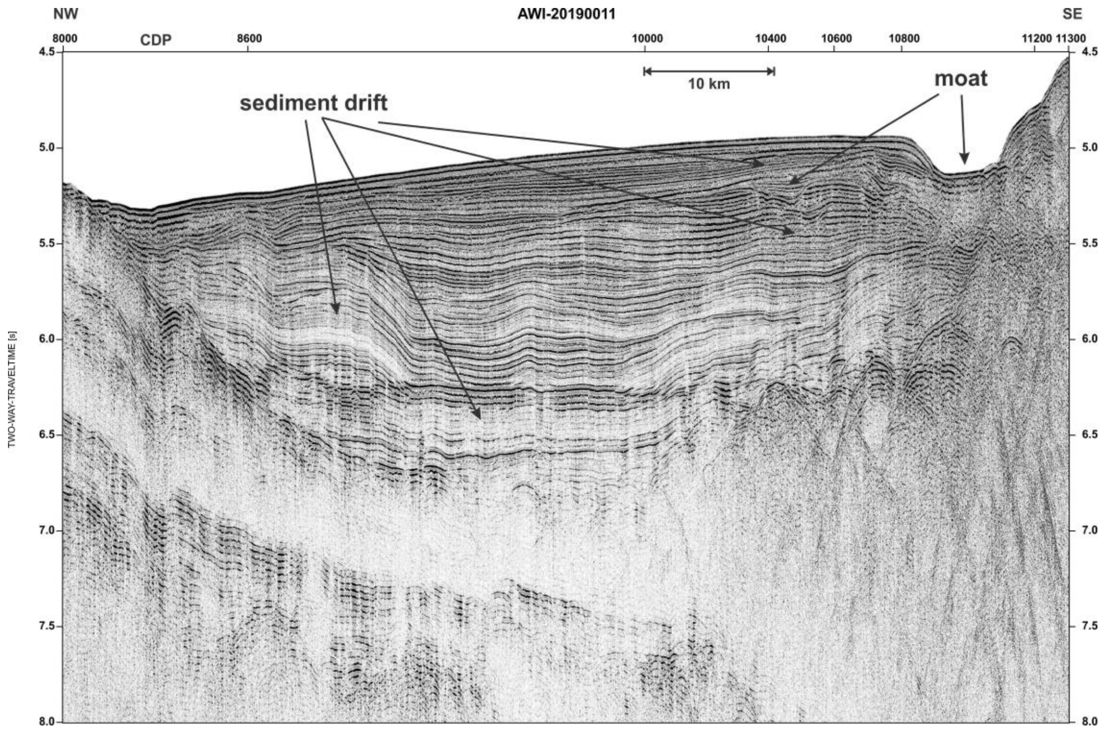

Fig. 5.6 Part of seismic reflection profile AWI-20190011 across the channel south of the Falkland Plateau. Several sediment drifts and moats can be observed.

The central Falkland Plateau in general shows erosion, especially the Paleogene/Neogene sequences appear to be affected strongly. Several phases of drift formation can be identified in the Palaeogene/Neogene sequences separated by erosional unconformities, which lie disconformably on the Maastrichtian horizon (Figs. 5.4 and 5.5). This is an indication for intensified current activity in Paleogene/Neogene times.

South of the Falkland Plateau a channel can be observed, which appears to have its base in the late Cretaceous (?) (Figs. 5.5 and 6.5). This channel is filled with sedimentary sequences, which have been shaped into sediment drifts. Those different drifts indicate a relocation of the shaping water mass (Fig. 5.6). Taking into account the water depth (~ 3800 m) the shaping water mass is suspected to be South Pacific Deepwater and/or Weddell Sea Deepwater.

As can be seen in Figs. 5.4. and 5.5., the Precambrian basement rises towards the Maurice Ewing Bank. A first interpretation of the seismic profiles collected across the MEB points towards a basement high, possibly a ridge, which underlies the bank. This high is wider in the West and narrower in the East. Sedimentary sequences are attached to the ridge from the North and the South. West of ~43° W a basin is formed north of the basement high. This basin is filled with sedimentary sequences, which are pulled-up and/or shaped into drifts (Fig. 5.7). The sequences are thin over the northern flank of the basement high, while another set of sediment drifts is formed attached from the South. The different depth ranges (above and below 2000 m), in which the sets of sediment drifts occur, point towards formation by UCDW (< 2000 m) and LCDW (> 2000 m), both obviously recirculated due to the topography of the MEB.

Summarising, the dataset is of excellent quality and images both tectonic structures as well as current controlled sedimentary features. Several lines of interpretation ranging from tectono-magmatic reactivation of the plateau in the late Cretaceous to activity and relocation of pathways of deep water masses are possible. This will provide further information about the development of this important part of the South Atlantic, where the tectonic development has had strong implications for the exchange of water masses and thus the development of the climate.

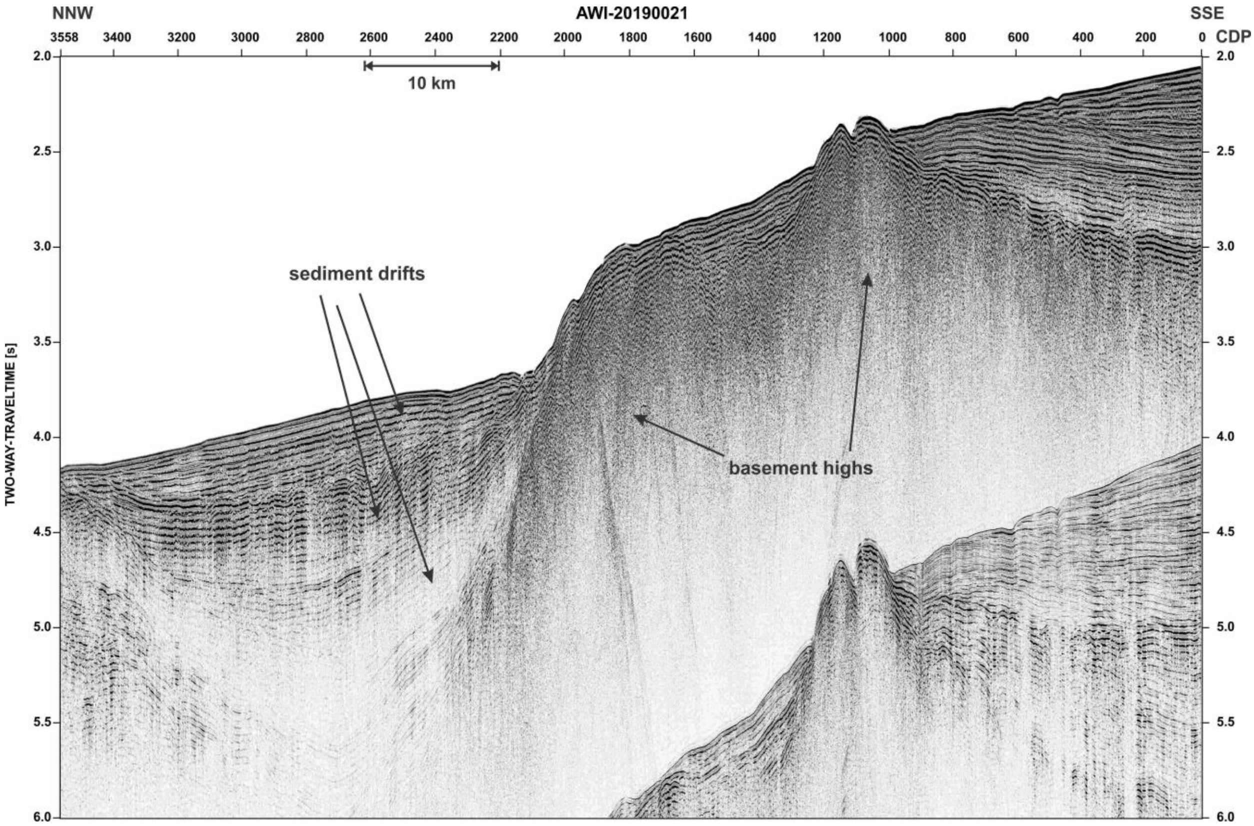

Fig. 5.7 Seismic reflection profile AWI-20190021 across northern Maurice Ewing Bank. Several sediment drifts can be observed.

5.2 Sediment Acoustics / Sub-Bottom Profiling

(T. Westerhold[1], A.-D. Ramadan[2], R. Reuter[2])
[1]MARUM
[2]AWI

During MSM81 cruise the parametric sub-bottom profiler PARASOUND was applied to image the upper 200m of sediment drape below the ship track.

5.2.1 Technical Description

The hull-mounted parametric echo sounder system PARASOUND™ DS3 (P70) was developed by TELEDYNE ATLAS HYDROGRAPHIC GmbH. In order to achieve high lateral resolution and image small-scale structures on the seafloor PARASOUND utilizes the parametric effect.

Simultaneously transmission of very high (finite) amplitude sound waves of slightly different frequencies, the primary high frequencies, will create harmonic sound waves at different low and high secondary frequencies. Advantage of this approach is that a secondary low frequency signal can travels within the narrow ~4.5° beam of the primary signal allowing a higher lateral resolution and imaging of small-scale structures on the seafloor superior to conventional systems. Directly emitting a low frequency signal with e.g. 4 kHz from the same transducer would produce a ~30° broad beam with much lower resolution. In the PARASOUND system a fixed Primary High Frequency (PHF) can be set between 18 and 33 kHz to form Secondary Low Frequency (SLF) signals with frequencies from 0.5 to 6.0 kHz. The parametric echo sounding transducer transmits highly linear signals with 70 kW transmission power to achieve a maximum penetration depth of about 200 m in soft sediments.

5.2.2 Data Acquisition

PARASOUND sub-bottom profiling data were acquired almost continuously from 09th of February, 21:34 UTC to the 10th of March 2019, 19:02 UTC. To generate a parametric sub-bottom profiler Secondary Low Frequency (SLF) of 4 kHz the first Primary High Frequency (PHF) was set to 19.8 kHz, resulting in a second PHF of ~23.8 kHz. The system was operated in quasi-equidistant pinging mode (multiple pulses in the water column) with 140 Volt Transmission Voltage, except for shallow shelf areas where single pulse mode was applied. Incoming data were stored in ASD-, SEGY- and PS3-files. PHF signal and rarely Kongsberg EM122 multibeam depth was used for seafloor detection.

Fig. 5.8 Facies type one: hummocky surface with up to 15 m of penetration on Falkland Plateau. Shown is

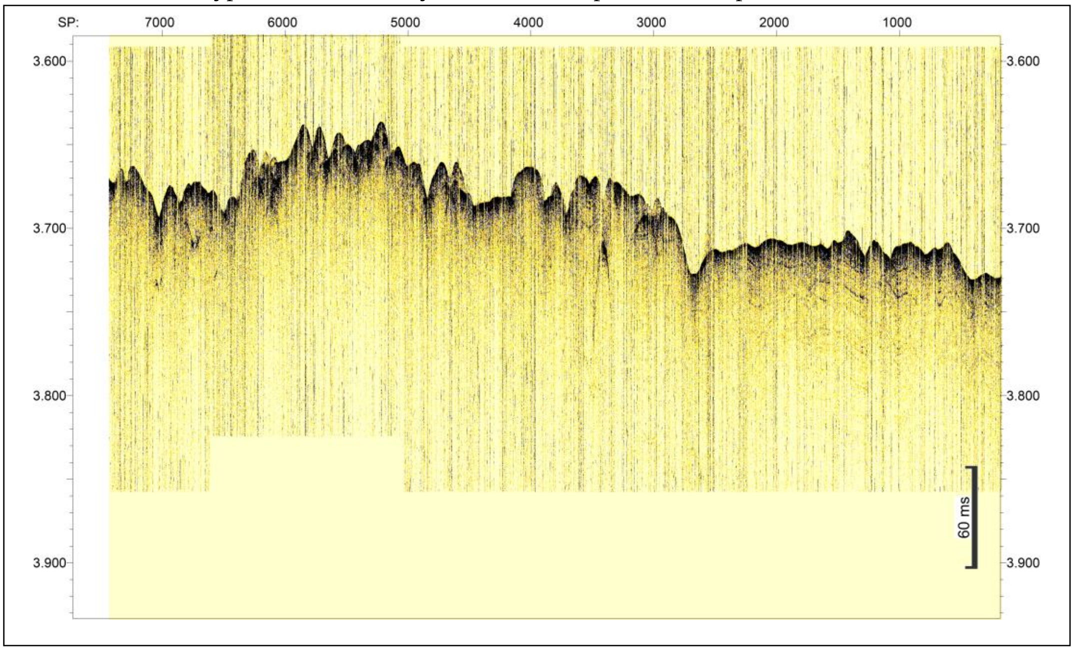

the SLF on seismic line AWI20190009 acquired on the 25th of February 2019 between 20:45 to 24:00 UTC (SP=shotpoint).

PARASOUND was switched off inside the 12 mile zone from 11.02.19 23:53 UTC to 12.02.19 03:36 UTC sailing in and out of Stanley for MedEvac. The system was switched to standby during deployment of a sound velocity profiler 13.02.19 00:54 UTC to 13.02.19 03:20 UTC. SLF data (4 kHz) were acquired during the entire cruise and stored both in ASD and PS3 format. PS3 data were then converted to *.sgy-files using the ps32sgy tool (written by Hanno Keil, University of Bremen) and imported into IHS Kingdom® for visualization and quality control.

5.2.3 Sediment Acoustics Preliminary Results

During MSM81, three different types of seismic facies were observed:

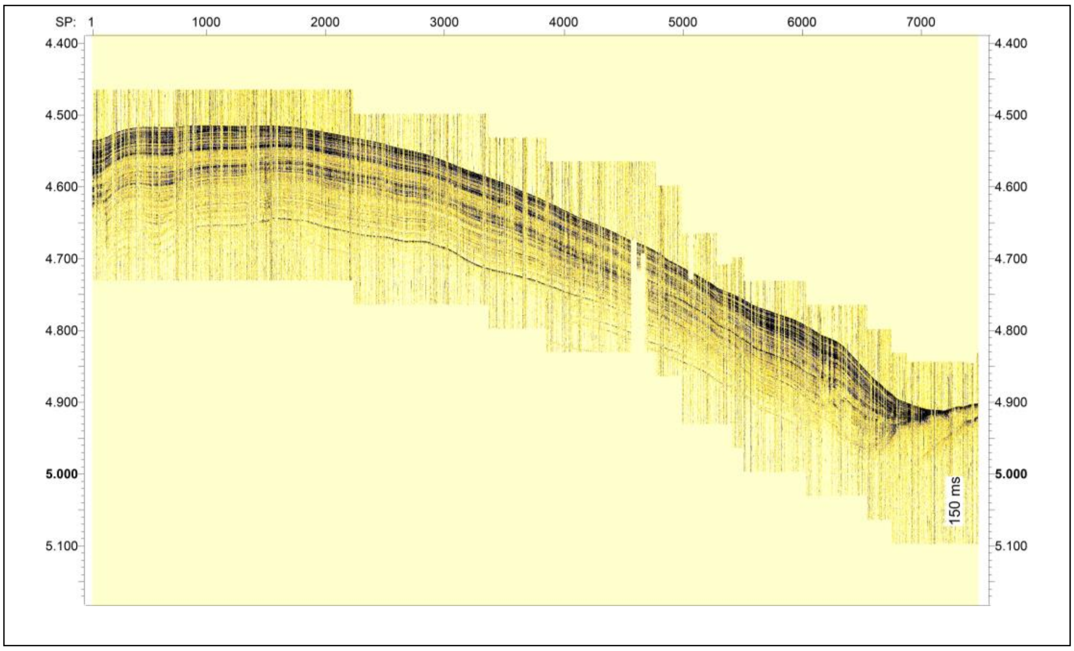

Fig. 5.9 Facies type two example: thick packages of planar sediment layers with more than 100 m of penetration in the Falkland Trough region. Shown is the SLF on seismic line AWI20190012 acquired on the 28th of February 2019 between 08:04 to 12:04 UTC.

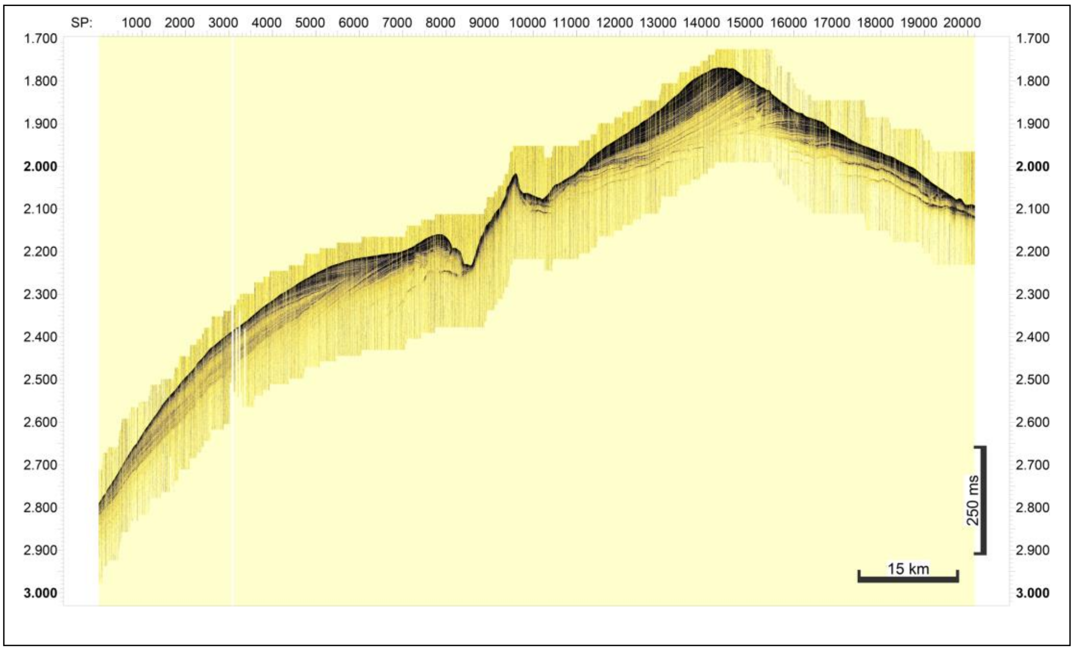

Fig. 5.10 Facies type three example: thick packages of planar sediment layers with discordant contact and deep of penetration on the southern flank of Maurice Ewing Bank. Shown is the SLF on seismic line AWI20190013 acquired on the 1st of March 2019.

Facies type one is characterized by low penetration of the PARASOUND signal. During MSM81 two varieties of low penetration have been observed: one with a hard surface with less than 10 m penetration, and another with a hummocky surface with up to 15 m of penetration (Fig. 5.8). The latter is commonly found on the Falkland Plateau area where sediment deposition was very low during the Neogene. Hard surfaces are observed at steeper slopes into the Falkland Trough and on the northern flank of Maurice Ewing Bank.

Facies type two consists of thick packages of planar sediment layers with deep penetration of the PARASOUND signal. This facies was observed in the Falkland Trough and the Northeastern Maurice Ewing Bank Basin where large drift sediment bodies with a penetration of more than 100 meters were encountered (Fig. 5.9).

Facies type three is characterized by deep penetration showing multiple generations of well layered sediment packages with discordant contacts. In some places slightly deformed sedimentary layers can be images by the subbottom profiler revealing tectonically related internal structures (Fig. 5.10). This facies type occurred mainly on the southern flank and on top of Maurice Ewing Bank.

5.3 Bathymetry

(J. Geils[1], S. Andree[1], L. Knopp[1])

[1]AWI

One of the most important measurements in marine science obviously is the water depth. For investigations of the water column, the seafloor and the subseafloor the size of the water body has to be known. To gain these values echosounders are used. The overall principle is quite simple. Acoustic energy is transmitted down through the water and the returning echo from the seafloor is recorded. The product of the sound velocity with the travel time gives the distances of the sounder to the seafloor (remember the signal travels through the water column twice). Speaking generally, one transmitter and one receiver are sufficient for the vertical ray path. This means one depth measurement vertically beneath the vessel. Such a device is a so called singlebeam echosounder (SBES). To derive more extensive information a more complex arrangement of transmitters and receivers needs to be used. These multibeam echosounders (MBES) are based on two transducer chains: one transmitting the acoustic pulse (aligned along the vessel), one receiving the echo (aligned across the vessel). Transmitting the signal with multiple transducers leads to interference within the water – a signal forms which is very narrow along ship and wide across ship. Due to this fact rays also leave the transducer under an angle. The point information of a SBES is augmented to a line information for a MBES (sampled discreetly). The incoming echos are then differentiated by the receiving transducer chain via time delays. A vessel moving forward can therefore map an area.

During cruise MSM81 bathymetry measurements were conducted due to add to the sparse MBES data on the Falkland Plateau. Furthermore, an exact depth information is very useful in combination with the acquired seismic data. For those reasons the measurements started at 9th February 2019 21:32 UTC and ended at the 13th of March 2019 22:00 UTC. The acquisition was continuous. Only for station work (SVP) or due to technical issues the devices was turned off shortly.

5.3.1 System Overview

On board on RV *MARIA S. MERIAN* the hull-mounted MBES Kongsberg EM122 was used. This deep sea echosounder has got a measuring range from 20 to 11000 m and uses frequencies from 11.25 to 12.6 kHz depending on the measuring sector. For one ping 864 depth values are calculated. The vertical resolution is 10 to 40 cm (theoretically) and horizontally 2° x 2° per beam. The transducers are, as mentioned above, aligned perpendicular to each other (mills cross) and have got a length of 8 m each. The time, position and motion data coming from the Kongsberg Seapath system is fed directly into the Processing Unit of the MBES. Based on that, the system is able to compensate Pitch and Yaw angles of 10° and Roll angles of 15° in real-time. The opening angle is up to 150°. However this angle was reduced to 130° in shallow water and 120° in deep water to get satisfactory results in the outer beams too. The MBES was operated with the software Seafloor Information System (SIS) from Kongsberg.

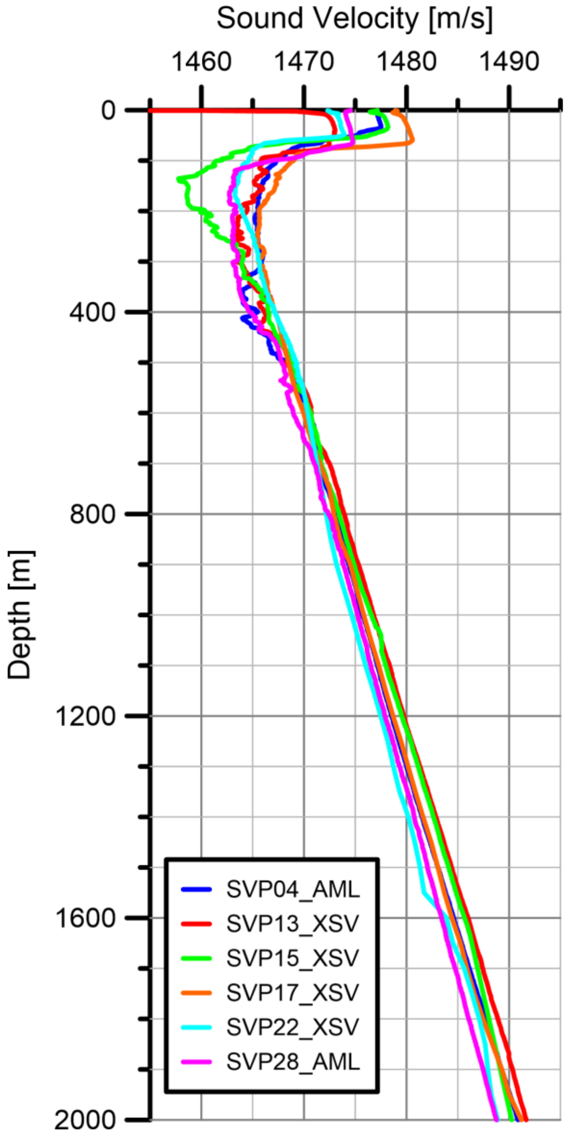

Fig. 5.11 Sound Velocity Profiles measured during MSM81. All profiles are extended to 12000 m water depth (necessary for SIS, v_{12000}=1675.8 m/s).

5.3.2 Sound Velocity Measurements

Apart from the echo travel time the sound velocity is the second important parameter to gain an exact depth value with a correct positioning. Starting with the vertical ray path but especially for the oblique ray paths (refraction within the water column, Snellius's law) this second information is mandatory. During MSM81 Sound Velocity Profiles (SVP's) were provided in three different ways.

The highest accuracy was achieved by the AML Applied Microsystems SV PlusX. This is a probe which measures the sound velocity directly via a small pinger while it is attached to a ship's wire with a forerunning weight. Therefore the ship has to be on station to retrieve an SVP. When not possible to stop, a SVP was provided via the Lockheed-Martin Sippican XSV. The single-use XSV is launched from the aft of the ship and provides online information of the sound speed via a glass-fibre wire while falling through the water column. For the transits to/from the working area and for the case that there was too much turbulence in water behind the vessel to launch an XSV, synthetic SVP's from the WorldOceanAtlas 2013 were used. Figure 5.11 shows the measured data (AML and XSV) during MSM81. The position and date of each SVP, also the synthetic ones, are listed in Table 5.3.

In order to handle the SVP's from different sources, the SoundSpeedManager (SSM) served as a platform. With the help of this program the profiles were smoothed and extended down to 12000 m (compulsory for SIS) and exported as .asvp. Subsequently, the profiles were applied in SIS.

Table 5.3 Sound Velocity Stations during MSM81.

Bathymetry Station	Official Station	Station Type	Date	UTC	Longitude [°]	Latitude [°]
SVP01	X	WOA13	2019-02-09	21:30	-60.00000000	-52.71666600
SVP02	X	WOA13	2019-02-11	07:15	-54.00000000	-52.71821667
SVP03	X	WOA13	2019-02-11	22:45	-56.00000000	-51.89085000
SVP04	MSM81_1-1	AML	2019-02-13	03:00	-50.70638330	-52.54156667
SVP05	MSM81_4-1	XSV	2019-02-14	22:00	-47.42805000	-51.19458333
SVP06	X	WOA13	2019-02-14	19:30	-46.97170000	-51.00470000
SVP07	X	WOA13	2019-02-16	04:30	-47.70697154	-50.25092205
SVP08	X	WOA13	2019-02-17	14:50	-48.88885065	-50.95042881
SVP09	X	WOA13	2019-02-18	10:20	-47.61580958	-52.53549768
SVP10	X	WOA13	2019-02-19	20:30	-46.94137501	-50.86856402
SVP11	X	WOA13	2019-02-20	21:00	-50.32665747	-50.99406128
SVP12	X	WOA13	2019-02-22	23:30	-49.19250480	-52.56101792
SVP13	MSM81_10-3	XSV	2019-02-23	00:00	-48.53106800	-51.60622700
SVP14	X	WOA13	2019-02-23	23:30	-47.63077865	-49.95550231
SVP15	MSM81_13-1	XSV	2019-02-24	17:00	-46.96865200	-51.00843100
SVP16	X	WOA13	2019-02-25	09:00	-48.18019730	-50.89039057
SVP17	MSM81_14-3	XSV	2019-02-26	12:00	-50.22333300	-51.01045600
SVP18	X	WOA13	2019-02-27	10:00	-48.46333262	-52.14896914
SVP19	X	WOA13	2019-02-28	08:00	-46.33065899	-52.76418987

SVP20	X	WOA13	2019-03-01	05:00	-44.68889049	-51.02892427
SVP21	X	WOA13	2019-03-02	14:00	-41.66173015	-49.91671343
SVP22	MSM81_21-3	XSV	2019-03-03	10:35	-42.38398400	-50.03378100
SVP23	X	WOA13	2019-03-04	23:30	-43.93392115	-49.81911390
SVP24	X	WOA13	2019-03-06	01:30	-44.50846826	-49.82613052
SVP25	X	WOA13	2019-03-07	06:00	-45.72196576	-49.88767716
SVP26	X	WOA13	2019-03-08	14:00	-46.97301033	-50.18429652
SVP27	X	WOA13	2019-03-08	23:30	-46.29933479	-49.81250829
SVP28	MSM81_35-1	AML	2019-03-10	22:30	-46.85360000	-50.21910300
SVP29	X	WOA13	2019-03-11	03:40	-47.47570156	-49.00101382
SVP30	X	WOA13	2019-03-12	08:00	-51.05920890	-40.91200242

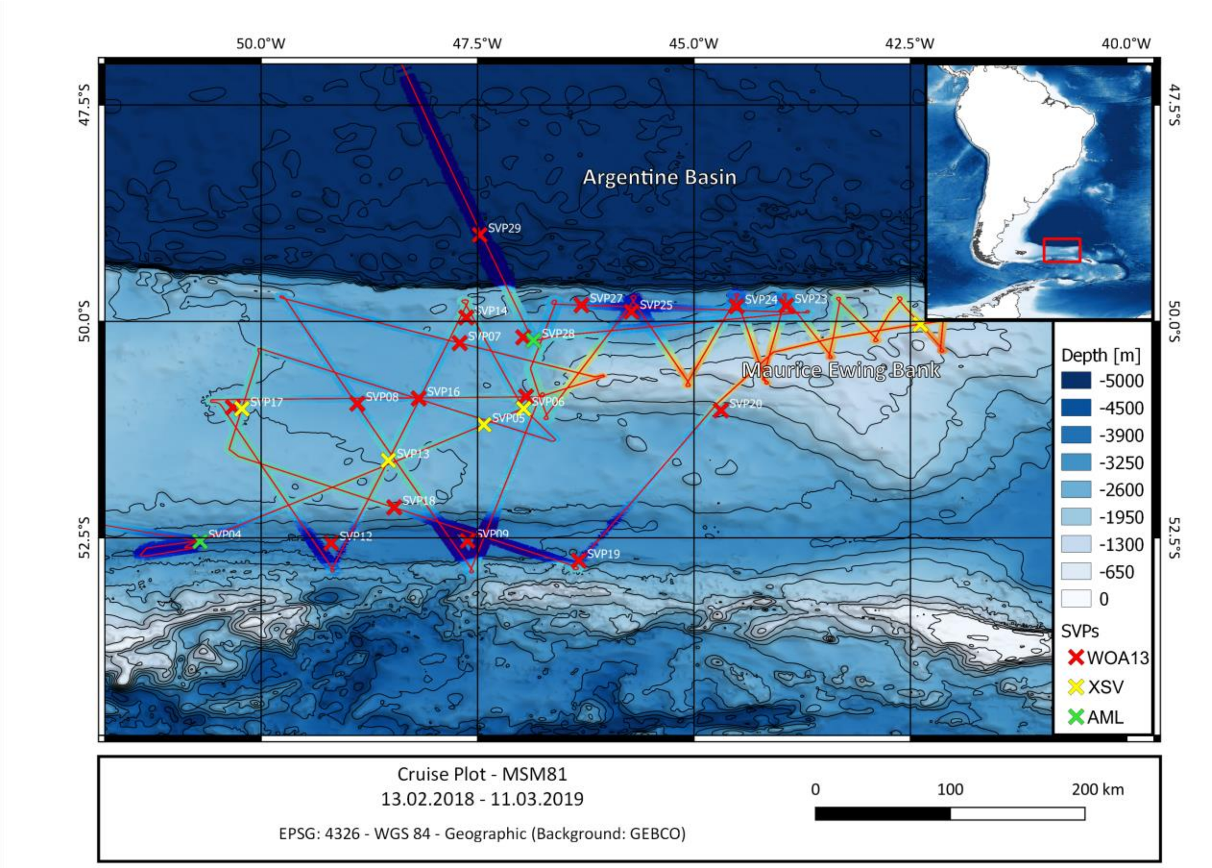

Fig. 5.12 MSM81 cruise plot. The acquired bathymetry, the position and type of SVP's and the cruise track are shown.

5.3.3 Data Processing

For the acquired bathymetrical data (Kongsberg .all files), a processing flow was started. After the import into CARIS Hips and Sips the data was again sound velocity corrected with the CARIS algorithm. To do so, a file containing all used SVP's is needed from the SSM. Then the algorithm uses the closest SVP for the correction. Afterwards, the across track position of each depth value has to be merged with the navigational data to obtain a geographical position for each depth measurement. After that preparation the actual processing can start. First, the data is swath edited to recognize and delete outliers. Secondly, the files are edited with the help of the subset editor, a type of 3D-editor, for a more precise examination of the data. After that, gridding with different cell sizes take place and the results can be exported.

To plot the data, plan the SVP's and to avoid doubling of MBES coverage with older cruises, the software QGIS was used.

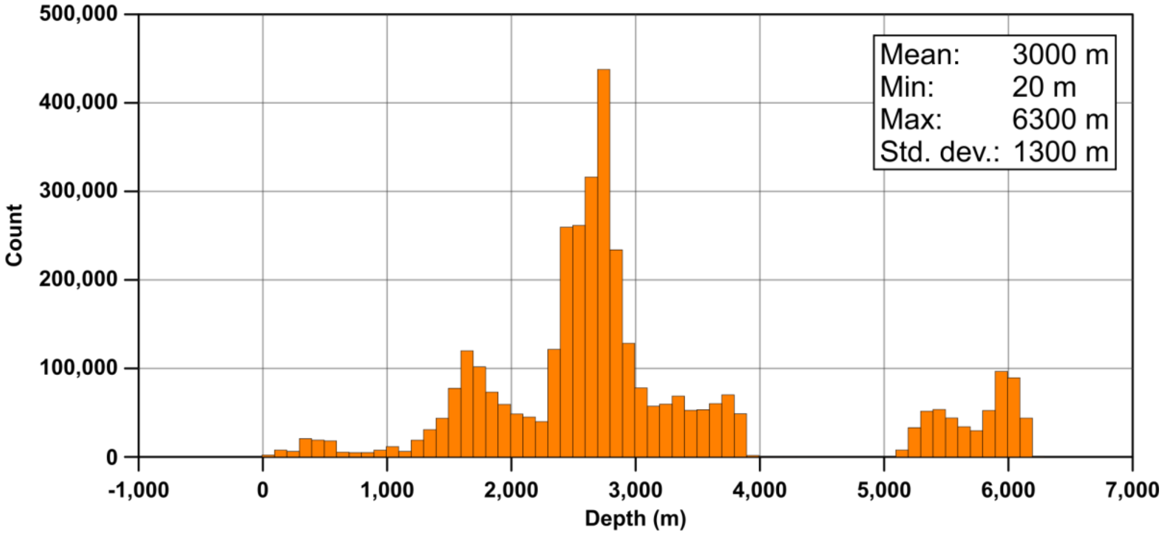

Fig. 5.13 Depth distribution during MSM81. Bining = 100 m. Note: the deep values from 5000 to 6000 m are measured while transit to Montevideo in the Argentine Basin.

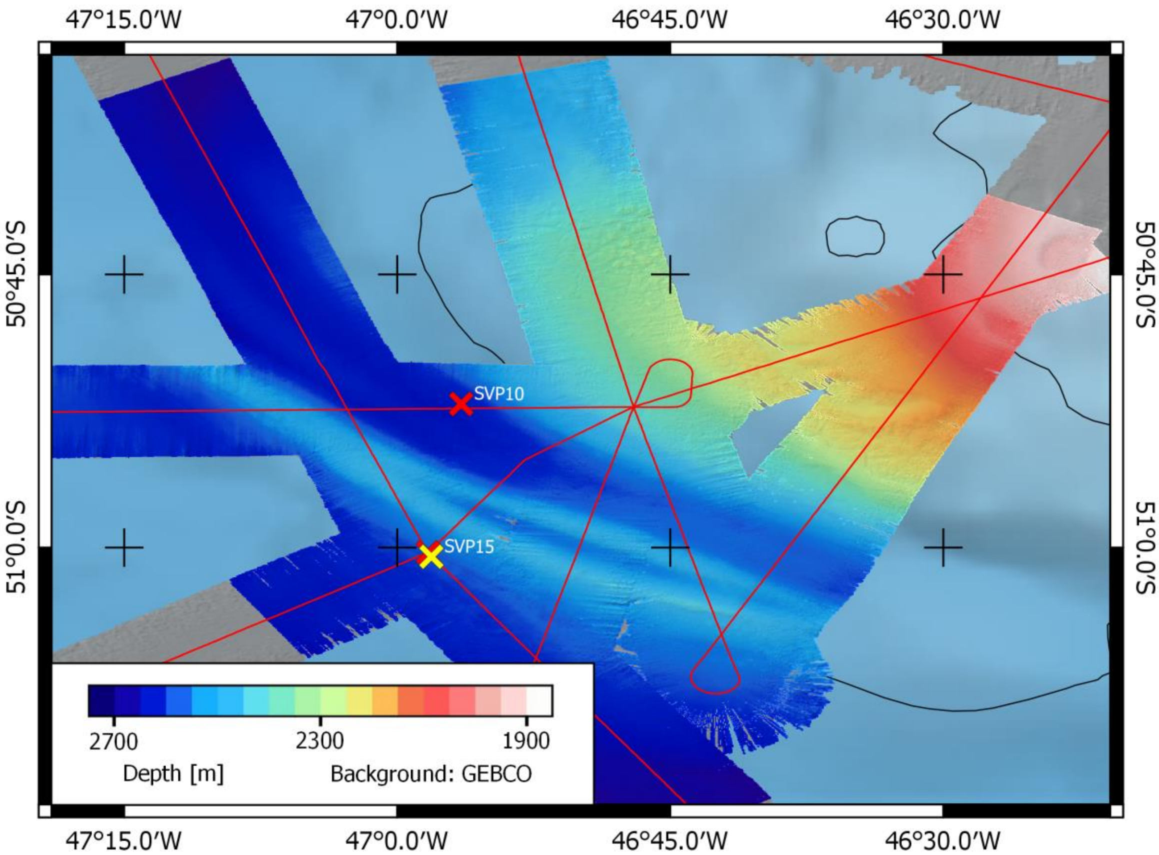

Fig. 5.14 Bathymetry of the "Barker Ridge" in the transition from the Maurice Ewing Bank (Northeast) to the plateau (Southwest).

As an example of an interesting feature mapped during the cruise, Figure 5.14 shows the "Barker Ridge" in the transition from the western Maurice Ewing Bank to the plateau. The data shows the structure to strike Northwest-Southeast and to be 50 km long (NW to SE), up to 13 km wide and about 200 m high. The middle part of the ridge shows two peaks in elevation. However, the northwest and southeast ends show only one bathymetrical high.

5.3.4 Preliminary Results

During MSM81 an area of about 150000 km² with a track length of about 8500 km was mapped. Figure 5.12 shows the cruise track with the acquired data, the SVP's and the GEBCO bathymetry in the working area. Figure 5.13 gives the depth distribution of the data. Also visible in this plot is the Falkland Plateau with its depths around 2400 to 3000 m. The second smaller peak from 1400 to 2000 m reflects the Maurice Ewing Bank. Depths values greater than 5000 m were acquired in the Argentine Basin.

6 Ship's Meteorological Station

There was no meteorologist on board during cruise MSM81.

7 Station List MSM81

(G. Uenzelmann-Neben)

7.1 Overall Station List

See Appendix A

7.2 Profile Station List

See Appendix B

8 Data and Sample Storage and Availability

All data collected during cruise MSM81 will form the base for a PhD project. This project will comprise the processing of the seismic data as well as the interpretation of the seismic, Parasound and multi-beam data to answer the questions raised under 3.1. A proposal has been handed in to the DFG priority programme IODP to acquire the funds for this PhD project.

The meta data for this cruise will be made publicly available immediately after the cruise. The raw and processed seismic data will be archived on the dedicated data server at AWI. Bathymetry and Parasound data as well as ADCP will be archived in PANGAEA.

Table 8.1 Overview of data availability

Type	Database	Available	Free Access	Contact
raw data ADCP	PANGAEA	Feb 2020	Feb 2021	gabriele.uenzelmann-neben@awi.de
multibeam	PANGAEA, BSH	Feb 2023	Feb 2024	gabriele.uenzelmann-neben@awi.de
Parasound	PANGAEA, BSH	Feb 2023	Feb 2024	gabriele.uenzelmann-neben@awi.de
seismic	AWI data archive	Feb 2023	Feb 2024	gabriele.uenzelmann-neben@awi.de

9 Acknowledgements

We like to thank Captain Ralf Schmidt, his officers and crew of RV *MARIA S. MERIAN* for their support of our measurement programme and for creating a very friendly atmosphere on board.

This cruise was provided by the Deutsche Forschungsgemeinschaft within the core programme METEOR/MERIAN. We also benefited from financial contributions by the research institutes involved. We gratefully acknowledge all this support.

10 References

Barker, P.F., Thomas, E., 2004. Origin, signature and palaeoclimatic influence of the Antarctic Circumpolar Current. Earth-Science Reviews 66, 143-166.

Ciesielski, P.F., Weaver, F.M., 1980. Neogene and Quaternary Paleoenvironmental history of Deep Sea Drilling Project Leg 71 Sediments, Southwest Atlantic Ocean. In: Ludwig, W.J., Krasheninnikov, V.A., et al. (Eds.), Initial Reports DSDP. U.S. Govt. Printing Office, Washington, pp. 461-477.

Coxall, H.K., Wilson, P.A., Paelike, H., Lear, C.H., Backmann, J., 2005. Rapid stepwise onset of Antarctic glaciation and deeper calcite compensation in the Pacific Ocean. Nature 433, 53-56.

DeConto, R.M., Pollard, D., Wilson, P.A., Pälike, H., Lear, C.H., Pagani, M., 2008. Thresholds for Cenozoic bipolar glaciation. Nature 455, 652-657.

Goldner, A., Herold, N., Huber, M., 2014. Antarctic glaciation caused ocean circulation changes at the Eocene-Oligocene transition. Nature 511 (7511), 574-577.

Koenitz, D., White, N., McCave, I.N., Hobbs, R., 2008. Internal structure of a contourite drift generated by the Antarctic Circumpolar Current. Geochemistry Geophysics Geosystems 9.

Livermore, R., Hillenbrand, C.-D., Meredith, M., Eagles, G., 2007. Drake Passage and Cenozoic climate: An open and shut case? Geochemistry Geophysics Geosystems 8.

Naveira Garabato, A.C., McDonagh, E.L., Stevens, D.P., Heywood, K.J., Sanders, R.J., 2002. On the export of Antarctic Bottom Water from the Weddell Sea. Deep Sea Research Part II: Topical Studies in Oceanography 49 (21), 4715-4742.

Pagani, M., Zachos, J.C., Freeman, K.H., Tipple, B., Bohaty, S., 2005. Marked Decline in Atmospheric Carbon Dioxide Concentrations During the Paleogene. Science 309 (5734), 600-603.

Pérez, L., Hernández-Molina, F.J., Esteban, F., Tassone, A., Piola, A., Maldonado, A., Preu, B., Violante, R., Lodolo, E., 2015. Erosional and depositional contourite features at the transition between the western Scotia Sea and southern South Atlantic Ocean: links with regional water-mass circulation since the Middle Miocene. Geo-Marine Letters 35 (4), 271-288.

Schlitzer, R., 2013. Ocean Data View. http://odv.awi.de.

Shipboard Scientific Party, 1977. Evolution of the Southwestern Atlantic Ocean Basin: Results of Leg 36, Deep Sea Drilling Project. In: Barker, P.F., Dalziel, I., Wise Jr, S.W., et al. (Eds.), Initial Reports DSDP. U.S. Govt. Printing Office, Washington, pp. 993-1014.

Shipboard Scientific Party, 1980. Site 511. In: Ludwig, W.J., Krasheninnikov, V.A., et al. (Eds.), Initial Reports DSDP. U.S. Govt. Printing Office, Washington, pp. 21-109.

Shipboard Scientific Party, 1988. Preliminary Results of Subantarctic South Atlantic Leg 114 of the Ocean Drilling Program. In: Ciesielski, P.F., Kristoffersen, Y., al., E. (Eds.), Proceedings of the Ocean Drilling Program, Initial Reports. US Government Printing, Washington, pp. 797-803.

Smith, W.H.S., Sandwell, D.T., 1997. Global Sea Floor Topography from Satellite Altimetry and Ship Depth Soundings. Science 277, 1956-1962.

Sokolov, S., Rintoul, S.R., 2009. Circumpolar structure and distribution of the Antarctic Circumpolar Current fronts: 1. Mean circumpolar paths. J. Geophys. Res. 114.

Uenzelmann-Neben, G., Weber, T., Grützner, J., Thomas, M., 2017. Transition from the Cretaceous ocean to Cenozoic circulation in the western South Atlantic — A twofold reconstruction. Tectonophysics 716 (Supplement C), 225-240.

Zachos, J.C., Pagani, M., Sloan, L., Thomas, E., Billups, K., 2001. Trends, Rhythms, and Aberrations in Global Climate 65 Ma to Present. Science 292, 686-693.

Appendices

Appendix A Stationbook MSM81

Activity No	Date / Time UTC	Device	Action	Position Lat	Position Lon	Depth [m]	Speed [kn]	Course [°]	Wind Direction [°]	Wind Velocity [m/s]	Winch	Rope Length [m]	Comment
MSM81_1-1	2/13/2019 1:07	Sound Velocity Profiler	in the water	52° 32,488' S	050° 42,336' W	3414.9	1	259	295	33.6	ERROR	0	
MSM81_1-1	2/13/2019 2:04	Sound Velocity Profiler	max depth/on ground	52° 32,588' S	050° 42,384' W	3421.1	1	215	279	38	EL2	3200	
MSM81_1-1	2/13/2019 3:01	Sound Velocity Profiler	on deck	52° 32,958' S	050° 42,394' W	3440.4	0	76	274	30.6	EL2	-16	
MSM81_2-1	2/13/2019 3:13	Deep-sea Multibeam Echosounder	profile start	52° 32,955' S	050° 42,389' W	3439.9	0	126	274	30.8	ERROR	0	Variable Kurse und Geschwindigkeiten (mit Parasound)
MSM81_2-1	2/13/2019 11:12	Deep-sea Multibeam Echosounder	profile end	52° 36,958' S	050° 45,608' W	3631.4	9	73	224	37.8	ERROR	0	
MSM81_3-1	2/13/2019 12:34	Seismic Towed Receiver	information	52° 34,717' S	050° 49,613' W	3526.7	4	49	229	39.5	ERROR	0	Beginn Ausstecken
MSM81_3-1	2/13/2019 14:33	Seismic Towed Receiver	MCS in water	52° 30,922' S	050° 39,263' W	3473.6	4	70	226	37.3	ERROR	0	Ausgesteckte Länge:3141m
MSM81_3-2	2/13/2019 14:54	Seismic Source	Gi-gun in water	52° 30,331' S	050° 37,564' W	3890.5	3	50	220	36.4	ERROR	0	Bb-Array, 2x GI-Guns
MSM81_3-2	2/13/2019 15:05	Seismic Source	information	52° 29,946' S	050° 36,579' W	3361.4	4	51	219	39.6	ERROR	0	Beginn Soft Start

Activity No	Date / Time UTC	Device	Action	Position Lat	Position Lon	Depth [m]	Speed [kn]	Course [°]	Wind Direction [°]	Wind Velocity [m/s]	Winch	Rope Length [m]	Comment
MSM81_3-2	2/13/2019 15:28	Seismic Source	information	52° 29,001' S	050° 34,257' W	3356.9	5	59	224	37.1	ERROR	0	Ende Soft Start
MSM81_3-2	2/13/2019 15:28	Seismic Source	profile start	52° 28,993' S	050° 34,239' W	3358	5	58	223	36.3	ERROR	0	v= 5,5kn; rwk 056°
MSM81_3-2	2/13/2019 16:19	Seismic Source	information	52° 26,795' S	050° 28,762' W	3258.2	5	50	227	36.7	ERROR	0	Überfahren geplanten Startpunkt
MSM81_4-1	2/14/2019 22:20	Expandedable Sound Velocimeter	in the water	51° 11,681' S	047° 25,697' W	2764.2	4	52	300	23.4	ERROR	0	Heckmitte zw. Gun u. Streamer
MSM81_4-1	2/14/2019 22:24	Expandedable Sound Velocimeter	station end	51° 11,552' S	047° 25,383' W	2759.8	4	65	298	23.4	ERROR	0	Sondendraht gekappt
MSM81_3-2	2/15/2019 3:20	Seismic Source	alter course	51° 00,187' S	046° 58,235' W	2584.4	4	31	289	26.1	ERROR	0	auf rwk 034°
MSM81_3-2	2/15/2019 3:23	Seismic Source	information	51° 00,010' S	046° 58,057' W	2573.4	4	39	287	25.9	ERROR	0	Überfahren WP DSDP_511 auf Profil
MSM81_3-2	2/15/2019 4:42	Seismic Source	alter course	50° 55,280' S	046° 53,087' W	2626.7	4	16	272	27.8	ERROR	0	auf rwk 052°
MSM81_3-2	2/15/2019 4:43	Seismic Source	information	50° 55,263' S	046° 53,069' W	2625.5	4	27	272	27.7	ERROR	0	Überfahren WP DSDP_330 auf Profil
MSM81_3-2	2/15/2019 5:50	Seismic Source	alter course	50° 52,319' S	046° 47,098' W	2788.7	4	63	275	31.4	ERROR	0	auf rwk 064°

Activity No	Date / Time UTC	Device	Action	Position Lat	Position Lon	Depth [m]	Speed [kn]	Course [°]	Wind Direction [°]	Wind Velocity [m/s]	Winch	Rope Length [m]	Comment
MSM81_3-2	2/15/2019 5:50	Seismic Source	information	50° 52,316' S	046° 47,091' W	2396.3	4	54	274	32	ERROR	0	Überfahren WP DSDP_327 auf Profil
MSM81_3-2	2/15/2019 11:46	Seismic Source	information	50° 39,214' S	046° 05,491' W	1512.3	5	67	234	31.1	ERROR	0	Überfahren WP 6
MSM81_3-2	2/15/2019 12:08	Seismic Source	profile end	50° 38,409' S	046° 03,002' W	1493.7	6	73	239	28.7	ERROR	0	
MSM81_3-1	2/15/2019 12:08	Seismic Towed Receiver	information	50° 38,399' S	046° 02,967' W	1490.9	6	62	240	28.7	ERROR	0	Profil end
MSM81_5-1	2/15/2019 12:48	Seismic Towed Receiver	information	50° 37,840' S	046° 05,698' W	1519.4	5	244	237	33.6	ERROR	0	Seismisches Equipment der Station MSM 81-3 noch ausgesteckt
MSM81_5-2	2/15/2019 12:48	Seismic Source	information	50° 37,841' S	046° 05,700' W	1518.6	5	254	237	33.6	ERROR	0	Seismisches Equipment der Station MSM 81-3 noch ausgesteckt
MSM81_5-2	2/15/2019 12:48	Seismic Source	profile start	50° 37,841' S	046° 05,701' W	1518.6	5	259	237	33.6	ERROR	0	v=5kn; rwk 250°
MSM81_5-2	2/15/2019 13:05	Seismic Source	alter course	50° 38,404' S	046° 07,895' W	1544.9	6	244	246	31.7	ERROR	0	auf rwk 291°
MSM81_5-2	2/16/2019 17:32	Seismic Source	information	49° 53,451' S	049° 07,928' W	2958.2	5	302	274	32.3	ERROR	0	Zugverbindung gebrochen, Streamer hängt nur noch an der Winde
MSM81_5-2	2/16/2019 18:00	Seismic Source	information	49° 52,940' S	049° 09,898' W	2957	2	294	276	30.4	ERROR	0	Zugverbindung wieder hergestellt

Activity No	Date / Time UTC	Device	Action	Position Lat	Position Lon	Depth [m]	Speed [kn]	Course [°]	Wind Direction [°]	Wind Velocity [m/s]	Winch	Rope Length [m]	Comment
MSM81_5-2	2/16/2019 22:56	Seismic Source	information	49° 44,454' S	049° 43,308' W	2768.9	4	292	250	27.7	ERROR	0	Überfahren WP Endpunkt Profil 2
MSM81_5-2	2/16/2019 23:24	Seismic Source	profile end	49° 43,648' S	049° 46,117' W	2748.4	4	307	246	25.5	ERROR	0	
MSM81_5-1	2/16/2019 23:24	Seismic Towed Receiver	information	49° 43,637' S	049° 46,150' W	2747.9	4	293	246	26	ERROR	0	Profil Ende
MSM81_6-1	2/16/2019 23:45	Seismic Towed Receiver	information	49° 42,431' S	049° 46,098' W	2739.3	6	114	248	22.4	ERROR	0	Seismisches Equipment der Station MSM 81-3 noch ausgesteckt.
MSM81_6-2	2/16/2019 23:45	Seismic Source	information	49° 42,438' S	049° 46,062' W	2738.4	6	99	247	22.6	ERROR	0	Seismisches Equipment der Station MSM 81-3 noch ausgesteckt.
MSM81_6-2	2/17/2019 0:04	Seismic Source	profile start	49° 43,579' S	049° 43,946' W	2750.8	6	142	253	23.7	ERROR	0	v=5kn; rwk 157°
MSM81_6-2	2/18/2019 18:36	Seismic Source	information	52° 51,387' S	047° 34,342' W	2640.7	5	154	195	13.4	ERROR	0	Überfahren WP Endpunkt Profil 3
MSM81_6-2	2/18/2019 19:00	Seismic Source	profile end	52° 53,181' S	047° 33,046' W	2701.2	5	162	196	16.6	ERROR	0	
MSM81_6-1	2/18/2019 19:01	Seismic Towed Receiver	information	52° 53,250' S	047° 33,000' W	2715.2	5	161	194	15.8	ERROR	0	Profil Ende
MSM81_7-1	2/18/2019 19:38	Seismic Towed Receiver	information	52° 53,163' S	047° 35,314' W	2733.3	5	20	189	20	ERROR	0	Seismisches Equipment der Station MSM 81-3 noch ausgesteckt

Activity No	Date / Time UTC	Device	Action	Position Lat	Position Lon	Depth [m]	Speed [kn]	Course [°]	Wind Direction [°]	Wind Velocity [m/s]	Winch	Rope Length [m]	Comment
MSM81_7-2	2/18/2019 19:38	Seismic Source	information	52° 53,118' S	047° 35,286' W	2721.1	5	21	189	19.9	ERROR	0	Seismisches Equipment der Station MSM 81-3 noch ausgesteckt.
MSM81_7-2	2/18/2019 19:38	Seismic Source	profile start	52° 53,110' S	047° 35,280' W	2721.1	5	27	189	19.9	ERROR	0	v=5,0kn; rwk 014°
MSM81_7-2	2/19/2019 20:52	Seismic Source	information	50° 52,276' S	046° 46,995' W	2397.2	5	8	260	17.2	ERROR	0	Überfahren WP Endpunkt Profil 4
MSM81_7-2	2/19/2019 21:16	Seismic Source	profile end	50° 50,333' S	046° 46,199' W	2341.4	5	18	270	18.2	ERROR	0	
MSM81_7-1	2/19/2019 21:16	Seismic Towed Receiver	information	50° 50,302' S	046° 46,186' W	2341.9	5	12	270	18	ERROR	0	profile end
MSM81_8-1	2/19/2019 21:54	Seismic Towed Receiver	information	50° 51,910' S	046° 43,973' W	2338.5	6	205	270	16.9	ERROR	0	Seismisches Equipment der Station MSM 81-3 noch ausgesteckt
MSM81_8-2	2/19/2019 21:54	Seismic Source	information	50° 51,910' S	046° 43,973' W	2338.5	6	205	270	16.9	ERROR	0	Seismisches Equipment der Station MSM 81-3 noch ausgesteckt
MSM81_8-2	2/19/2019 21:55	Seismic Source	profile start	50° 51,911' S	046° 43,975' W	2338.5	6	206	270	16.9	ERROR	0	v=5kn; rwk 269°
MSM81_8-2	2/21/2019 3:04	Seismic Source	information	50° 54,278' S	050° 30,381' W	2544.2	5	259	307	28	ERROR	0	Überfahren WP Profil 5
MSM81_8-2	2/21/2019 3:29	Seismic Source	profile end	50° 54,311' S	050° 33,574' W	2537	5	279	307	24.9	ERROR	0	

Activity No	Date / Time UTC	Device	Action	Position Lat	Position Lon	Depth [m]	Speed [kn]	Course [°]	Wind Direction [°]	Wind Velocity [m/s]	Winch	Rope Length [m]	Comment
MSM81_8-1	2/21/2019 3:29	Seismic Towed Receiver	information	50° 54,310' S	050° 33,606' W	2533.4	5	274	306	25.1	ERROR	0	profile end
MSM81_9-1	2/21/2019 4:09	Seismic Towed Receiver	information	50° 56,107' S	050° 32,859' W	2515.1	5	91	312	25.1	ERROR	0	Seismisches Equipment der Station MSM 81-3 noch ausgesteckt
MSM81_9-2	2/21/2019 4:09	Seismic Source	information	50° 56,107' S	050° 32,851' W	2515.1	6	88	312	25.1	ERROR	0	Seismisches Equipment der Station MSM 81-3 noch ausgesteckt
MSM81_9-2	2/21/2019 4:09	Seismic Source	profile start	50° 56,107' S	050° 32,849' W	2500.8	6	87	311	25.2	ERROR	0	v=5,0kn; rwk 157°
MSM81_9-2	2/21/2019 21:20	Seismic Source	information	52° 09,964' S	049° 39,201' W	2576.8	5	152	222	28.4	ERROR	0	GI-Guns deaktiviert, Profilunterbrechung
MSM81_9-2	2/21/2019 21:32	Seismic Source	information	52° 10,784' S	049° 38,645' W	2593.3	4	154	222	27.3	ERROR	0	Gi-Guns an Deck für Wartung und Austausch Schleppdraht
MSM81_9-2	2/21/2019 23:15	Seismic Source	information	52° 17,984' S	049° 33,690' W	2906	5	155	219	32.9	ERROR	0	Beginn Soft Start
MSM81_9-2	2/21/2019 23:38	Seismic Source	information	52° 19,600' S	049° 32,575' W	3113.1	4	164	231	29.9	ERROR	0	Ende Soft Start
MSM81_9-2	2/21/2019 23:39	Seismic Source	information	52° 19,658' S	049° 32,545' W	3116.3	5	155	225	28.3	ERROR	0	Profil Fortsetzung v=5kn; rwk 157°
MSM81_9-2	2/22/2019 6:55	Seismic Source	information	52° 51,120' S	049° 10,699' W	2965.9	5	157	237	27.9	ERROR	0	Überfahren WP Ende Profil 6

Activity No	Date / Time UTC	Device	Action	Position Lat	Position Lon	Depth [m]	Speed [kn]	Course [°]	Wind Direction [°]	Wind Velocity [m/s]	Winch	Rope Length [m]	Comment
MSM81_9-1	2/22/2019 7:20	Seismic Towed Receiver	information	52° 52,959' S	049° 09,449' W	3002.6	4	152	242	24.5	ERROR	0	Profil end
MSM81_9-2	2/22/2019 7:20	Seismic Source	profile end	52° 52,966' S	049° 09,444' W	3013.9	4	153	241	24.6	ERROR	0	
MSM81_10-2	2/22/2019 7:58	Seismic Source	information	52° 52,411' S	049° 11,531' W	2971.3	6	7	248	25	ERROR	0	Seismisches Equipment der Station MSM 81-9 noch ausgesteckt
MSM81_10-2	2/22/2019 7:58	Seismic Source	profile start	52° 52,409' S	049° 11,531' W	2971.3	6	10	248	25	ERROR	0	v=5,0kn; rwk 018°
MSM81_10-1	2/22/2019 7:58	Seismic Towed Receiver	information	52° 52,346' S	049° 11,503' W	2977.3	5	22	247	24.5	ERROR	0	Seismisches Equipment der Station MSM 81-3 noch ausgesteckt
MSM81_10-3	2/22/2019 23:57	Expandedable Sound Velocimeter	in the water	51° 36,988' S	048° 32,197' W	2407.9	5	17	257	27.4	ERROR	0	
MSM81_10-3	2/23/2019 0:05	Expandedable Sound Velocimeter	station end	51° 36,374' S	048° 31,864' W	2429	5	13	256	26.3	ERROR	0	
MSM81_10-2	2/23/2019 23:13	Seismic Source	information	49° 48,948' S	047° 37,898' W	2420.5	5	33	303	6.1	ERROR	0	Überfahren WP auf dem Profil
MSM81_11-1	2/23/2019 23:35	Seismic Towed Receiver	information	49° 47,331' S	047° 37,097' W	2429.3	5	15	293	5.7	ERROR	0	Seismisches Equipment der Station MSM 81-3 noch ausgesteckt
MSM81_10-1	2/23/2019 23:40	Seismic Towed Receiver	information	49° 47,008' S	047° 36,950' W	2429	5	27	281	6.2	ERROR	0	Profil end

Activity No	Date / Time UTC	Device	Action	Position Lat	Position Lon	Depth [m]	Speed [kn]	Course [°]	Wind Direction [°]	Wind Velocity [m/s]	Winch	Rope Length [m]	Comment
MSM81_10-2	2/23/2019 23:40	Seismic Source	profile end	49° 46,978' S	047° 36,934' W	2430.7	5	3	280	6.5	ERROR	0	
MSM81_11-2	2/23/2019 23:47	Seismic Source	information	49° 46,403' S	047° 36,701' W	2431.4	4	26	275	4.7	ERROR	0	GI-Guns vorgehievt und drucklos
MSM81_11-2	2/24/2019 0:05	Seismic Source	information	49° 45,258' S	047° 37,375' W	2447.7	5	293	262	4.3	ERROR	0	GI-Guns ausgesteckt und unter Druck
MSM81_11-2	2/24/2019 0:39	Seismic Source	information	49° 46,125' S	047° 40,825' W	2451.1	6	180	266	3.3	ERROR	0	Beginn Soft Start
MSM81_11-2	2/24/2019 0:59	Seismic Source	information	49° 47,471' S	047° 38,999' W	2453.5	5	142	241	2.6	ERROR	0	Ende Soft Start
MSM81_11-2	2/24/2019 1:00	Seismic Source	profile start	49° 47,534' S	047° 38,923' W	2456.7	5	147	250	2.7	ERROR	0	v=5kn; rwk 161°
MSM81_11-2	2/24/2019 17:06	Seismic Source	alter course	51° 00,081' S	046° 58,441' W	2582.3	5	156	133	33.8	ERROR	0	auf rwk 147°
MSM81_11-2	2/24/2019 17:08	Seismic Source	information	51° 00,248' S	046° 58,338' W	2583.6	5	155	135	35.4	ERROR	0	Überfahren Wegpunkt DSDP_511
MSM81_12-1	2/24/2019 17:11	Expandedable Sound Velocimeter	in the water	51° 00,506' S	046° 58,119' W	2589.6	5	151	135	33.8	ERROR	0	
MSM81_12-1	2/24/2019 17:19	Expandedable Sound Velocimeter	station end	51° 01,035' S	046° 57,569' W	2585.6	5	143	137	32.4	ERROR	0	Ende Messung
MSM81_11-2	2/24/2019 22:24	Seismic Source	profile end	51° 21,452' S	046° 36,520' W	2759.8	5	161	167	33.7	ERROR	0	

Activity No	Date / Time UTC	Device	Action	Position Lat	Position Lon	Depth [m]	Speed [kn]	Course [°]	Wind Direction [°]	Wind Velocity [m/s]	Winch	Rope Length [m]	Comment
MSM81_11-1	2/24/2019 22:25	Seismic Towed Receiver	information	51° 21,480' S	046° 36,498' W	2761.7	5	152	167	34.8	ERROR	0	Profil end
MSM81_13-1	2/24/2019 22:55	Seismic Towed Receiver	information	51° 22,993' S	046° 39,189' W	2764.5	6	297	173	38.3	ERROR	0	Seismisches Equipment der Station MSM 81-3 noch ausgesteckt
MSM81_13-2	2/24/2019 22:55	Seismic Source	information	51° 22,992' S	046° 39,194' W	2764.5	6	300	173	38.3	ERROR	0	Seismisches Equipment der Station MSM 81-11 noch ausgesteckt
MSM81_13-2	2/24/2019 22:55	Seismic Source	profile start	51° 22,989' S	046° 39,200' W	2764.5	6	301	173	38.3	ERROR	0	v= 5kn; rwk 297°
MSM81_13-2	2/26/2019 2:39	Seismic Source	information	50° 18,996' S	050° 00,365' W	2536.5	6	286	190	30.9	ERROR	0	Überfahren WP auf Profil
MSM81_13-2	2/26/2019 2:40	Seismic Source	profile end	50° 18,977' S	050° 00,431' W	2537.1	5	297	192	31.3	ERROR	0	
MSM81_13-1	2/26/2019 2:42	Seismic Towed Receiver	information	50° 18,898' S	050° 00,701' W	2608.1	6	279	193	33.2	ERROR	0	Profil Ende
MSM81_14-1	2/26/2019 2:42	Seismic Towed Receiver	information	50° 18,881' S	050° 00,772' W	2536.8	5	281	197	35.1	ERROR	0	Seismisches Equipment der Station MSM 81-3 noch ausgesteckt
MSM81_14-2	2/26/2019 2:43	Seismic Source	information	50° 18,851' S	050° 00,939' W	2532.9	6	283	205	32.9	ERROR	0	Seismisches Equipment der Station MSM 81-11 noch ausgesteckt
MSM81_14-2	2/26/2019 3:05	Seismic Source	profile start	50° 20,192' S	050° 02,048' W	2500.5	6	161	201	29.2	ERROR	0	v=5kn; rwk 191°

Activity No	Date / Time UTC	Device	Action	Position Lat	Position Lon	Depth [m]	Speed [kn]	Course [°]	Wind Direction [°]	Wind Velocity [m/s]	Winch	Rope Length [m]	Comment
MSM81_14-2	2/26/2019 4:45	Seismic Source	information	50° 28,578' S	050° 03,344' W	2480.7	5	169	198	35.4	ERROR	0	Profil unterbrochen wegen techn. Probleme Kompressoren
MSM81_14-2	2/26/2019 5:38	Seismic Source	information	50° 33,089' S	050° 04,771' W	2489.4	5	190	186	24.2	ERROR	0	Auftriebsblasen der GI-Guns abgerissen.
MSM81_14-2	2/26/2019 6:39	Seismic Source	Gi-gun on deck	50° 38,098' S	050° 06,295' W	2509.4	4	188	199	27.1	ERROR	0	Gi-Guns zur Wartung an Deck
MSM81_14-2	2/26/2019 7:35	Seismic Source	Gi-gun in water	50° 41,780' S	050° 07,465' W	2507.9	3	184	203	27.1	ERROR	0	GI-Guns nach Wartung wieder zu Wasser
MSM81_14-2	2/26/2019 7:39	Seismic Source	information	50° 42,015' S	050° 07,504' W	2782.3	3	184	216	30.2	ERROR	0	Beginn Soft-Start.
MSM81_14-2	2/26/2019 8:00	Seismic Source	information	50° 43,425' S	050° 07,982' W	2502.6	4	189	210	25	ERROR	0	Ende Soft-Start, Fortsetzung Profil v=5kn; rwk 191°
MSM81_14-2	2/26/2019 8:50	Seismic Source	information	50° 47,160' S	050° 09,183' W	2515.7	5	187	217	25	ERROR	0	Auftriebsblasen abgerissen, Profilunterbrechung, Stop der GI-Guns, Beginn Pre-Watch.
MSM81_14-2	2/26/2019 9:08	Seismic Source	Gi-gun on deck	50° 48,341' S	050° 09,517' W	2513.7	4	230	207	26.9	ERROR	0	
MSM81_14-2	2/26/2019 9:50	Seismic Source	Gi-gun in water	50° 51,041' S	050° 10,350' W	2511.1	4	199	207	27.9	ERROR	0	
MSM81_14-2	2/26/2019 9:56	Seismic Source	information	50° 51,357' S	050° 10,462' W	2516.7	4	201	207	27.5	ERROR	0	Beginnn Soft-Start

Activity No	Date / Time UTC	Device	Action	Position Lat	Position Lon	Depth [m]	Speed [kn]	Course [°]	Wind Direction [°]	Wind Velocity [m/s]	Winch	Rope Length [m]	Comment
MSM81_14-2	2/26/2019 10:17	Seismic Source	information	50° 52,698' S	050° 10,908' W	2521.7	4	199	214	25.9	ERROR	0	Ende Soft-Start, Fortsetzung Profil v=5kn; rwk 191°
MSM81_14-3	2/26/2019 12:00	Expandedable Sound Velocimeter	in the water	51° 00,347' S	050° 13,337' W	2569.3	4	184	216	20.2	ERROR	0	
MSM81_14-3	2/26/2019 12:03	Expandedable Sound Velocimeter	station end	51° 00,520' S	050° 13,378' W	2563.4	4	214	212	22.5	ERROR	0	Ende Messung
MSM81_14-2	2/26/2019 18:00	Seismic Source	information	51° 28,304' S	050° 22,163' W	2315.8	5	191	265	16.1	ERROR	0	Ende Profil
MSM81_14-1	2/26/2019 18:00	Seismic Towed Receiver	information	51° 28,321' S	050° 22,169' W	2310.8	5	193	262	16.1	ERROR	0	Ende Profil
MSM81_15-1	2/26/2019 18:07	Seismic Towed Receiver	information	51° 28,916' S	050° 22,071' W	2322.1	6	155	267	16.6	ERROR	0	Seismisches Equipment der Station MSM 81-3 noch ausgesteckt
MSM81_15-2	2/26/2019 18:08	Seismic Source	Gi-gun on deck	51° 29,051' S	050° 21,946' W	2315.5	6	143	269	15.4	ERROR	0	GI-Guns an Deck
MSM81_15-2	2/26/2019 18:35	Seismic Source	Gi-gun in water	51° 30,660' S	050° 19,652' W	2320.5	4	154	265	18.9	ERROR	0	
MSM81_15-2	2/26/2019 19:00	Seismic Source	information	51° 32,126' S	050° 17,712' W	2319.1	5	136	267	18.5	ERROR	0	Beginn Soft-Start
MSM81_15-2	2/26/2019 19:00	Seismic Source	information	51° 32,132' S	050° 17,705' W	2319.1	5	156	267	18.5	ERROR	0	Ende Soft-Start

Activity No	Date / Time UTC	Device	Action	Position Lat	Position Lon	Depth [m]	Speed [kn]	Course [°]	Wind Direction [°]	Wind Velocity [m/s]	Winch	Rope Length [m]	Comment
MSM81_15-2	2/26/2019 19:20	Seismic Source	profile start	51° 33,431' S	050° 16,082' W	2329.4	5	140	265	20.8	ERROR	0	v=5kn; rwk 118°
MSM81_15-2	2/28/2019 4:00	Seismic Source	profile end	52° 50,210' S	046° 21,084' W	2652.8	5	124	169	32.8	ERROR	0	
MSM81_15-1	2/28/2019 4:00	Seismic Towed Receiver	information	52° 50,218' S	046° 21,058' W	2651.9	5	119	169	32.2	ERROR	0	Profil Ende
MSM81_16-1	2/28/2019 4:39	Seismic Towed Receiver	information	52° 52,028' S	046° 22,784' W	2645.8	6	290	182	37.2	ERROR	0	Seismisches Equipment der Station MSM 81-3 noch ausgesteckt
MSM81_16-2	2/28/2019 4:39	Seismic Source	information	52° 52,025' S	046° 22,795' W	2649.7	5	301	182	37.2	ERROR	0	Seismisches Equipment der Station MSM 81-15 noch ausgesteckt
MSM81_16-2	2/28/2019 4:40	Seismic Source	profile start	52° 51,981' S	046° 22,910' W	2652.2	5	302	180	36.9	ERROR	0	v=5,0kn; rwk 028°
MSM81_16-2	2/28/2019 5:09	Seismic Source	information	52° 49,726' S	046° 22,354' W	2733.3	5	35	182	30.1	ERROR	0	Überfahren WP Start Profil 12
MSM81_16-1	3/1/2019 6:13	Seismic Towed Receiver	information	50° 57,246' S	044° 44,270' W	2092.5	5	24	245	32	ERROR	0	Ende Profil
MSM81_16-2	3/1/2019 6:13	Seismic Source	profile end	50° 57,223' S	044° 44,250' W	2056.3	5	31	246	31.6	ERROR	0	
MSM81_17-1	3/1/2019 6:13	Seismic Towed Receiver	information	50° 57,220' S	044° 44,247' W	2056.3	5	27	246	31.6	ERROR	0	Seismisches Equipment der Station MSM 81-3 noch ausgesteckt

Activity No	Date / Time UTC	Device	Action	Position Lat	Position Lon	Depth [m]	Speed [kn]	Course [°]	Wind Direction [°]	Wind Velocity [m/s]	Winch	Rope Length [m]	Comment
MSM81_17-2	3/1/2019 6:14	Seismic Source	information	50° 57,144' S	044° 44,183' W	2168.2	5	28	247	29.7	ERROR	0	Seismisches Equipment der Station MSM 81-15 noch ausgesteckt
MSM81_17-2	3/1/2019 6:14	Seismic Source	profile start	50° 57,143' S	044° 44,182' W	2168.2	5	25	247	29.7	ERROR	0	v=5,0kn; rwk 035°
MSM81_17-2	3/1/2019 14:44	Seismic Source	profile end	50° 21,468' S	044° 05,170' W	1531	4	36	227	29.9	ERROR	0	
MSM81_17-1	3/1/2019 14:45	Seismic Towed Receiver	information	50° 21,435' S	044° 05,136' W	1651.1	5	29	228	29.9	ERROR	0	Ende Profil
MSM81_18-1	3/1/2019 14:49	Seismic Towed Receiver	information	50° 21,229' S	044° 04,831' W	1540.2	4	58	222	31	ERROR	0	Seismisches Equipment der Station MSM 81-3 noch ausgesteckt
MSM81_18-2	3/1/2019 14:58	Seismic Source	Gi-gun on deck	50° 21,060' S	044° 03,924' W	1544.7	4	84	220	28.2	ERROR	0	
MSM81_18-2	3/1/2019 15:20	Seismic Source	Gi-gun in water	50° 20,667' S	044° 01,831' W	1705.9	4	69	229	25.2	ERROR	0	
MSM81_18-2	3/1/2019 15:45	Seismic Source	information	50° 19,972' S	043° 58,819' W	1573.3	5	65	228	29.6	ERROR	0	Beginn Soft-Start
MSM81_18-2	3/1/2019 16:05	Seismic Source	information	50° 19,350' S	043° 56,211' W	1580.3	5	70	216	31	ERROR	0	Ende Soft Start
MSM81_18-2	3/1/2019 16:05	Seismic Source	profile start	50° 19,349' S	043° 56,202' W	1580.3	5	76	217	31.5	ERROR	0	v=5,0kn; rwk=070°

Activity No	Date / Time UTC	Device	Action	Position Lat	Position Lon	Depth [m]	Speed [kn]	Course [°]	Wind Direction [°]	Wind Velocity [m/s]	Winch	Rope Length [m]	Comment
MSM81_18-2	3/1/2019 20:41	Seismic Source	alter course	50° 11,589' S	043° 23,712' W	1729.7	5	76	228	24.9	ERROR	0	rwk 076°; Schiff überfährt WP auf Profil
MSM81_18-2	3/2/2019 2:56	Seismic Source	alter course	50° 04,009' S	042° 37,543' W	1579.2	5	71	226	27.5	ERROR	0	rwk 077°; Überfahren WP auf dem Profil
MSM81_18-2	3/2/2019 6:32	Seismic Source	alter course	50° 00,122' S	042° 10,892' W	1687.8	5	81	234	20.6	ERROR	0	rwk 081°; Schiff überfährt WP auf Profil
MSM81_18-2	3/2/2019 13:32	Seismic Source	information	49° 54,724' S	041° 18,546' W	1684.3	5	94	224	16.4	ERROR	0	Überfahren WP auf dem Profil
MSM81_18-2	3/2/2019 13:56	Seismic Source	profile end	49° 54,417' S	041° 15,554' W	1690	5	89	219	15.8	ERROR	0	
MSM81_18-1	3/2/2019 13:57	Seismic Towed Receiver	information	49° 54,400' S	041° 15,396' W	1693.5	5	82	219	16.5	ERROR	0	Ende Profil
MSM81_19-2	3/2/2019 14:36	Seismic Source	information	49° 55,644' S	041° 14,752' W	1675.4	6	288	253	15.5	ERROR	0	Seismisches Equipment der Station MSM 81-18 noch ausgesteckt
MSM81_19-2	3/2/2019 14:36	Seismic Source	profile start	49° 55,643' S	041° 14,756' W	1675.4	5	291	253	15.5	ERROR	0	v=5,0kn; rwk=286°
MSM81_19-1	3/2/2019 14:36	Seismic Towed Receiver	information	49° 55,638' S	041° 14,780' W	1675.8	5	284	252	15.2	ERROR	0	Seismisches Equipment der Station MSM 81-3 noch ausgesteckt
MSM81_19-2	3/2/2019 15:06	Seismic Source	information	49° 54,693' S	041° 18,542' W	1683	5	293	238	17.3	ERROR	0	Überfahren WP auf dem Profil

Activity No	Date / Time UTC	Device	Action	Position Lat	Position Lon	Depth [m]	Speed [kn]	Course [°]	Wind Direction [°]	Wind Velocity [m/s]	Winch	Rope Length [m]	Comment
MSM81_19-2	3/2/2019 18:16	Seismic Source	information	49° 50,330' S	041° 42,086' W	1693.3	5	285	212	12.3	ERROR	0	Überfahren WP auf dem Profil
MSM81_19-2	3/2/2019 20:01	Seismic Source	information	49° 47,975' S	041° 55,134' W	1773.5	5	281	212	9.6	ERROR	0	Profilunterbrechung, GI-Guns zur Reperatur an Deck
MSM81_19-2	3/2/2019 20:14	Seismic Source	Gi-gun on deck	49° 47,735' S	041° 56,465' W	1778.9	4	280	211	9.1	ERROR	0	
MSM81_19-1	3/2/2019 20:14	Seismic Towed Receiver	information	49° 47,729' S	041° 56,498' W	1777.2	4	294	209	9.2	ERROR	0	Profile end
MSM81_20-1	3/2/2019 21:53	Seismic Towed Receiver	information	49° 45,792' S	042° 07,268' W	1957.6	5	279	197	9.1	ERROR	0	
MSM81_20-2	3/2/2019 21:53	Seismic Source	Gi-gun in water	49° 45,782' S	042° 07,327' W	1960	5	287	200	9.2	ERROR	0	
MSM81_20-2	3/2/2019 22:03	Seismic Source	information	49° 45,478' S	042° 08,581' W	1984.8	5	300	190	8.8	ERROR	0	Beginn Soft-Start
MSM81_20-2	3/2/2019 22:23	Seismic Source	information	49° 44,188' S	042° 08,072' W	1996.5	5	80	182	7.2	ERROR	0	Ende Soft-Start
MSM81_20-2	3/2/2019 22:23	Seismic Source	profile start	49° 44,185' S	042° 08,035' W	1994.6	5	77	181	7.4	ERROR	0	v=5kn; rwk 183°
MSM81_20-2	3/3/2019 5:26	Seismic Source	information	50° 17,778' S	042° 09,019' W	1311.1	5	181	122	6.8	ERROR	0	Überfahren WP Profil
MSM81_20-2	3/3/2019 5:51	Seismic Source	profile end	50° 19,796' S	042° 09,200' W	1342.4	5	179	120	8.6	ERROR	0	

Activity No	Date / Time UTC	Device	Action	Position Lat	Position Lon	Depth [m]	Speed [kn]	Course [°]	Wind Direction [°]	Wind Velocity [m/s]	Winch	Rope Length [m]	Comment
MSM81_20-1	3/3/2019 5:51	Seismic Towed Receiver	information	50° 19,808' S	042° 09,201' W	1341.5	5	178	120	8.5	ERROR	0	Profil Ende
MSM81_21-1	3/3/2019 5:53	Seismic Towed Receiver	information	50° 19,963' S	042° 09,251' W	1341.7	6	198	121	8.8	ERROR	0	Seismisches Equipment der Station MSM 81-3 noch ausgesteckt
MSM81_21-2	3/3/2019 5:54	Seismic Source	information	50° 20,018' S	042° 09,282' W	1342.4	6	201	125	8.5	ERROR	0	Seismisches Equipment der Station MSM 81-20 noch ausgesteckt
MSM81_21-2	3/3/2019 6:30	Seismic Source	profile start	50° 20,058' S	042° 06,976' W	1342.9	6	340	130	9.6	ERROR	0	v=5,0kn; rwk=330°
MSM81_21-2	3/3/2019 7:00	Seismic Source	information	50° 17,759' S	042° 08,988' W	1311	5	334	124	9.5	ERROR	0	Überfahren WP auf Profil
MSM81_21-3	3/3/2019 10:34	Expandedable Sound Velocimeter	in the water	50° 02,008' S	042° 23,054' W	1655.4	5	336	111	10.8	ERROR	0	
MSM81_21-3	3/3/2019 10:37	Expandedable Sound Velocimeter	station end	50° 01,799' S	042° 23,231' W	1662.4	5	331	116	10.8	ERROR	0	
MSM81_21-1	3/3/2019 14:41	Seismic Towed Receiver	information	49° 44,286' S	042° 38,855' W	1997.1	5	333	93	8.1	ERROR	0	Ende Profil
MSM81_21-2	3/3/2019 14:41	Seismic Source	profile end	49° 44,223' S	042° 38,906' W	1999.3	5	333	92	7.8	ERROR	0	
MSM81_22-1	3/3/2019 14:46	Seismic Towed Receiver	information	49° 43,878' S	042° 39,026' W	2003.2	5	3	99	7.4	ERROR	0	Seismisches Equipment der Station MSM 81-3 noch ausgesteckt

Activity No	Date / Time UTC	Device	Action	Position Lat	Position Lon	Depth [m]	Speed [kn]	Course [°]	Wind Direction [°]	Wind Velocity [m/s]	Winch	Rope Length [m]	Comment
MSM81_22-2	3/3/2019 14:47	Seismic Source	information	49° 43,772' S	042° 39,010' W	2005.5	5	11	101	7.3	ERROR	0	Seismisches Equipment der Station MSM 81-20 noch ausgesteckt
MSM81_22-2	3/3/2019 15:20	Seismic Source	profile start	49° 44,267' S	042° 35,901' W	2060.8	6	183	89	7.7	ERROR	0	v=5kn; rwk 210°
MSM81_22-2	3/3/2019 17:35	Seismic Source	information	49° 54,159' S	042° 44,384' W	1789	6	204	113	7.1	ERROR	0	Überfahren WP auf dem Profil; ä/K auf rwK 200°
MSM81_22-1	3/3/2019 21:38	Seismic Towed Receiver	information	50° 13,084' S	042° 55,330' W	1580.9	5	197	101	6.2	ERROR	0	Profile end
MSM81_22-2	3/3/2019 21:38	Seismic Source	profile end	50° 13,107' S	042° 55,342' W	1580	5	194	100	6.2	ERROR	0	
MSM81_23-1	3/3/2019 22:17	Seismic Towed Receiver	information	50° 12,758' S	042° 52,700' W	1560.7	6	334	69	2.1	ERROR	0	Seismisches Equipment der Station MSM 81-3 noch ausgesteckt
MSM81_23-2	3/3/2019 22:17	Seismic Source	information	50° 12,758' S	042° 52,700' W	1560.7	6	334	69	2.1	ERROR	0	Seismisches Equipment der Station MSM 81-20 noch ausgesteckt
MSM81_23-2	3/3/2019 22:17	Seismic Source	profile start	50° 12,756' S	042° 52,701' W	1560.7	6	337	69	2.1	ERROR	0	v=5kn; rwK 327°
MSM81_23-2	3/4/2019 4:57	Seismic Source	profile end	49° 44,780' S	043° 20,732' W	2198.5	5	329	350	6.3	ERROR	0	
MSM81_23-1	3/4/2019 4:57	Seismic Towed Receiver	information	49° 44,760' S	043° 20,752' W	2195.1	5	327	349	7.3	ERROR	0	Profil Ende

Activity No	Date / Time UTC	Device	Action	Position Lat	Position Lon	Depth [m]	Speed [kn]	Course [°]	Wind Direction [°]	Wind Velocity [m/s]	Winch	Rope Length [m]	Comment
MSM81_24-1	3/4/2019 4:58	Seismic Towed Receiver	information	49° 44,707' S	043° 20,806' W	2195.1	5	327	349	7.5	ERROR	0	Seismisches Equipment der Station MSM 81-3 noch ausgesteckt
MSM81_24-2	3/4/2019 4:59	Seismic Source	information	49° 44,658' S	043° 20,853' W	2196	5	328	350	7.6	ERROR	0	Seismisches Equipment der Station MSM 81-20 noch ausgesteckt
MSM81_24-2	3/4/2019 5:35	Seismic Source	profile start	49° 44,469' S	043° 18,623' W	2144.8	6	187	16	6.1	ERROR	0	v=5kn; rwk 178°
MSM81_24-2	3/4/2019 11:03	Seismic Source	information	50° 11,595' S	043° 23,603' W	1731.1	5	189	4	18.6	ERROR	0	Überfahren WP 20_1 auf dem Profil
MSM81_24-1	3/4/2019 13:41	Seismic Towed Receiver	information	50° 24,610' S	043° 26,591' W	1439.6	5	189	14	21.9	ERROR	0	Ende Profil
MSM81_24-2	3/4/2019 13:41	Seismic Source	profile end	50° 24,656' S	043° 26,603' W	1439.8	5	192	16	21	ERROR	0	
MSM81_25-1	3/4/2019 13:46	Seismic Towed Receiver	information	50° 25,060' S	043° 26,572' W	1431.7	5	162	15	22.2	ERROR	0	Seismisches Equipment der Station MSM 81-3 noch ausgesteckt
MSM81_25-2	3/4/2019 13:47	Seismic Source	information	50° 25,104' S	043° 26,547' W	1428.9	5	159	16	22.2	ERROR	0	Seismisches Equipment der Station MSM 81-20 noch ausgesteckt
MSM81_25-2	3/4/2019 14:17	Seismic Source	profile start	50° 24,216' S	043° 24,673' W	1445.9	6	331	17	22.4	ERROR	0	v=5kn; rwk 330°
MSM81_25-1	3/4/2019 23:47	Seismic Towed Receiver	information	49° 42,106' S	043° 58,170' W	3018.8	5	331	2	24.9	ERROR	0	Ende Profil

Activity No	Date / Time UTC	Device	Action	Position Lat	Position Lon	Depth [m]	Speed [kn]	Course [°]	Wind Direction [°]	Wind Velocity [m/s]	Winch	Rope Length [m]	Comment
MSM81_25-2	3/4/2019 23:47	Seismic Source	profile end	49° 42,052' S	043° 58,217' W	3014.9	5	329	1	25.2	ERROR	0	
MSM81_26-1	3/4/2019 23:51	Seismic Towed Receiver	information	49° 41,812' S	043° 58,354' W	3007	5	348	359	25.1	ERROR	0	Seismisches Equipment der Station MSM 81-3 noch ausgesteckt
MSM81_26-2	3/4/2019 23:52	Seismic Source	information	49° 41,723' S	043° 58,371' W	3001.7	5	350	359	24.7	ERROR	0	Seismisches Equipment der Station MSM 81-20 noch ausgesteckt
MSM81_26-2	3/5/2019 0:21	Seismic Source	profile start	49° 41,814' S	043° 56,179' W	3011.9	5	194	356	23.2	ERROR	0	v=5kn; rwk 190°
MSM81_26-2	3/5/2019 12:10	Seismic Source	profile end	50° 39,880' S	044° 12,360' W	1489.6	5	203	18	37.8	ERROR	0	
MSM81_26-1	3/5/2019 12:10	Seismic Towed Receiver	information	50° 39,901' S	044° 12,367' W	1492.9	5	180	17	36.7	ERROR	0	Ende Profil
MSM81_27-1	3/5/2019 13:02	Seismic Towed Receiver	information	50° 43,201' S	044° 08,679' W	1553	5	224	12	38.6	ERROR	0	Seismisches Equipment der Station MSM 81-3 noch ausgesteckt
MSM81_27-2	3/5/2019 13:03	Seismic Source	information	50° 43,243' S	044° 08,748' W	1552.7	5	223	14	40.6	ERROR	0	Seismisches Equipment der Station MSM 81-20 noch ausgesteckt
MSM81_27-2	3/5/2019 13:30	Seismic Source	information	50° 42,414' S	044° 10,619' W	1542	4	354	17	37.7	ERROR	0	Beginn Soft Start
MSM81_27-2	3/5/2019 13:51	Seismic Source	information	50° 41,016' S	044° 10,662' W	1503.4	4	356	15	38.8	ERROR	0	Ende Soft Start

Activity No	Date / Time UTC	Device	Action	Position Lat	Position Lon	Depth [m]	Speed [kn]	Course [°]	Wind Direction [°]	Wind Velocity [m/s]	Winch	Rope Length [m]	Comment
MSM81_27-2	3/5/2019 14:02	Seismic Source	profile start	50° 40,204' S	044° 10,845' W	1497.7	5	343	18	37.6	ERROR	0	v=5kn; rwk 347°
MSM81_27-1	3/6/2019 2:29	Seismic Towed Receiver	information	49° 41,859' S	044° 31,482' W	3163.4	5	339	311	20	ERROR	0	Ende Profil
MSM81_27-2	3/6/2019 2:29	Seismic Source	profile end	49° 41,839' S	044° 31,493' W	3161.9	5	348	311	19.8	ERROR	0	
MSM81_28-1	3/6/2019 2:30	Seismic Towed Receiver	information	49° 41,724' S	044° 31,543' W	3166.2	5	349	309	19.9	ERROR	0	Seismisches Equipment der Station MSM 81-3 noch ausgesteckt
MSM81_28-2	3/6/2019 2:31	Seismic Source	information	49° 41,675' S	044° 31,557' W	3169.1	5	354	309	19.6	ERROR	0	Seismisches Equipment der Station MSM 81-20 noch ausgesteckt
MSM81_28-2	3/6/2019 3:07	Seismic Source	profile start	49° 41,813' S	044° 29,194' W	3141.2	6	199	312	20.1	ERROR	0	v=5kn; rwk 200°
MSM81_28-2	3/6/2019 15:58	Seismic Source	profile end	50° 41,853' S	045° 04,175' W	1571.6	5	197	343	20.8	ERROR	0	
MSM81_28-1	3/6/2019 15:58	Seismic Towed Receiver	information	50° 41,864' S	045° 04,182' W	1573	5	202	342	20.9	ERROR	0	Prifile end
MSM81_29-1	3/6/2019 16:04	Seismic Towed Receiver	information	50° 42,238' S	045° 04,408' W	1573.8	4	201	346	20.2	ERROR	0	Seismisches Equipment der Station MSM 81-3 noch ausgesteckt
MSM81_29-2	3/6/2019 16:16	Seismic Source	Gi-gun on deck	50° 42,875' S	045° 04,789' W	1583.7	4	208	343	20.8	ERROR	0	Guns zur Wartung an Deck

Activity No	Date / Time UTC	Device	Action	Position Lat	Position Lon	Depth [m]	Speed [kn]	Course [°]	Wind Direction [°]	Wind Velocity [m/s]	Winch	Rope Length [m]	Comment
MSM81_29-2	3/6/2019 17:27	Seismic Source	Gi-gun in water	50° 43,492' S	045° 03,144' W	1590.1	4	344	347	26.1	ERROR	0	
MSM81_29-2	3/6/2019 17:29	Seismic Source	information	50° 43,371' S	045° 03,218' W	1593	4	334	344	26.5	ERROR	0	Beginn Soft-Start
MSM81_29-2	3/6/2019 17:49	Seismic Source	information	50° 41,817' S	045° 04,151' W	1577.2	5	331	343	27.9	ERROR	0	End Soft-Start
MSM81_29-2	3/6/2019 17:50	Seismic Source	profile start	50° 41,760' S	045° 04,184' W	1570.8	5	341	343	27.7	ERROR	0	v=5kn: rwk 336°
MSM81_29-2	3/7/2019 6:50	Seismic Source	profile end	49° 44,113' S	045° 43,327' W	3482.9	5	334	328	34.6	ERROR	0	
MSM81_29-1	3/7/2019 6:50	Seismic Towed Receiver	information	49° 44,096' S	045° 43,339' W	3483.5	5	337	329	34.1	ERROR	0	Profil Ende
MSM81_30-1	3/7/2019 6:50	Seismic Towed Receiver	information	49° 44,047' S	045° 43,372' W	3488.5	5	333	328	32.9	ERROR	0	Seismisches Equipment der Station MSM 81-3 noch ausgesteckt
MSM81_30-2	3/7/2019 6:51	Seismic Source	information	49° 43,994' S	045° 43,407' W	3491.1	5	342	327	33.8	ERROR	0	Seismisches Equipment der Station MSM 81-29 noch ausgesteckt
MSM81_30-2	3/7/2019 7:28	Seismic Source	profile start	49° 42,418' S	045° 40,820' W	3679.3	6	122	331	35.3	ERROR	0	v=5,0kn; rwk=206°
MSM81_30-1	3/8/2019 2:22	Seismic Towed Receiver	information	51° 06,645' S	046° 43,672' W	2573.3	5	210	226	14.1	ERROR	0	Ende Profil

Activity No	Date / Time UTC	Device	Action	Position Lat	Position Lon	Depth [m]	Speed [kn]	Course [°]	Wind Direction [°]	Wind Velocity [m/s]	Winch	Rope Length [m]	Comment
MSM81_30-2	3/8/2019 2:22	Seismic Source	profile end	51° 06,678' S	046° 43,700' W	2573.8	5	193	225	13.9	ERROR	0	
MSM81_31-1	3/8/2019 2:26	Seismic Towed Receiver	information	51° 07,010' S	046° 43,846' W	2587.6	5	193	239	13.1	ERROR	0	Seismisches Equipment der Station MSM 81-3 noch ausgesteckt
MSM81_31-2	3/8/2019 2:27	Seismic Source	information	51° 07,049' S	046° 43,853' W	2587.6	5	179	244	12.1	ERROR	0	Seismisches Equipment der Station MSM 81-29 noch ausgesteckt
MSM81_31-2	3/8/2019 3:01	Seismic Source	profile start	51° 07,010' S	046° 41,252' W	2575.4	5	339	245	12.9	ERROR	0	v=5,0kn; rwk=346°
MSM81_31-2	3/8/2019 6:02	Seismic Source	alter course	50° 52,256' S	046° 47,020' W	2396	5	349	257	9	ERROR	0	Neuer Kurs rwk=348°, Überfahren WP DSDP_327
MSM81_31-2	3/8/2019 9:59	Seismic Source	profile end	50° 32,949' S	046° 53,343' W	2512.8	5	351	235	14.1	ERROR	0	
MSM81_31-1	3/8/2019 9:59	Seismic Towed Receiver	information	50° 32,938' S	046° 53,346' W	2514.7	5	345	235	14	ERROR	0	Profil end
MSM81_32-1	3/8/2019 9:59	Seismic Towed Receiver	information	50° 32,925' S	046° 53,350' W	2514	5	346	235	13.9	ERROR	0	Seismisches Equipment der Station MSM 81-3 noch ausgesteckt
MSM81_32-2	3/8/2019 9:59	Seismic Source	information	50° 32,925' S	046° 53,350' W	2514	5	346	235	13.9	ERROR	0	Seismisches Equipment der Station MSM 81-29 noch ausgesteckt

Activity No	Date / Time UTC	Device	Action	Position Lat	Position Lon	Depth [m]	Speed [kn]	Course [°]	Wind Direction [°]	Wind Velocity [m/s]	Winch	Rope Length [m]	Comment
MSM81_32-2	3/8/2019 9:59	Seismic Source	profile start	50° 32,924' S	046° 53,351' W	2514	5	344	235	13.9	ERROR	0	v=5kn; rwk 014°
MSM81_32-2	3/8/2019 19:43	Seismic Source	profile end	49° 46,271' S	046° 35,455' W	2846.7	5	9	212	20.8	ERROR	0	
MSM81_32-1	3/8/2019 19:43	Seismic Towed Receiver	information	49° 46,243' S	046° 35,447' W	2845	5	10	213	20.8	ERROR	0	Profile end
MSM81_33-1	3/8/2019 20:22	Seismic Towed Receiver	information	49° 46,943' S	046° 38,586' W	2836.1	5	210	209	19.5	ERROR	0	Seismisches Equipment der Station MSM 81-3 noch ausgesteckt
MSM81_33-2	3/8/2019 20:22	Seismic Source	information	49° 46,945' S	046° 38,587' W	2836.1	5	207	209	19.5	ERROR	0	Seismisches Equipment der Station MSM 81-29 noch ausgesteckt
MSM81_33-2	3/8/2019 20:22	Seismic Source	profile start	49° 46,946' S	046° 38,588' W	2836.1	5	203	209	19.5	ERROR	0	v=5kn; rwk 093°
MSM81_33-2	3/9/2019 18:34	Seismic Source	profile end	49° 53,968' S	043° 42,362' W	2696.2	5	92	254	24.8	ERROR	0	
MSM81_33-1	3/9/2019 18:34	Seismic Towed Receiver	information	49° 53,971' S	043° 42,311' W	2696.2	5	88	255	24.2	ERROR	0	Profile end
MSM81_34-1	3/9/2019 19:12	Seismic Towed Receiver	information	49° 52,601' S	043° 41,744' W	2698.3	5	231	253	25.8	ERROR	0	Seismisches Equipment der Station MSM 81-3 noch ausgesteckt
MSM81_34-2	3/9/2019 19:12	Seismic Source	information	49° 52,602' S	043° 41,745' W	2698.3	5	230	253	25.8	ERROR	0	Seismisches Equipment der Station MSM 81-29 noch ausgesteckt

Activity No	Date / Time UTC	Device	Action	Position Lat	Position Lon	Depth [m]	Speed [kn]	Course [°]	Wind Direction [°]	Wind Velocity [m/s]	Winch	Rope Length [m]	Comment
MSM81_34-2	3/9/2019 19:12	Seismic Source	profile start	49° 52,604' S	043° 41,749' W	2698.3	5	246	253	25.8	ERROR	0	v=5kn rwk 262°
MSM81_34-2	3/10/2019 19:00	Seismic Source	profile end	50° 10,137' S	046° 36,375' W	2642.1	4	271	239	17.5	ERROR	0	
MSM81_34-1	3/10/2019 19:00	Seismic Towed Receiver	information	50° 10,138' S	046° 36,384' W	2642.1	4	255	239	17.4	ERROR	0	Profile end
MSM81_34-1	3/10/2019 19:05	Seismic Towed Receiver	information	50° 10,215' S	046° 36,750' W	2642.1	3	246	243	15.4	ERROR	0	Beginn Einholen Streamer
MSM81_34-2	3/10/2019 19:15	Seismic Source	Gi-gun on deck	50° 10,399' S	046° 37,453' W	2631	4	247	250	14	ERROR	0	
MSM81_34-1	3/10/2019 21:57	Seismic Towed Receiver	MCS on deck	50° 13,122' S	046° 51,095' W	2753	3	245	268	16.9	ERROR	0	
MSM81_35-1	3/10/2019 22:06	Sound Velocity Profiler	in the water	50° 13,146' S	046° 51,216' W	2750.1	0	45	272	16.3	EL1	0	
MSM81_35-1	3/10/2019 22:51	Sound Velocity Profiler	max depth/on ground	50° 13,147' S	046° 51,215' W	2751.3	0	231	284	15	EL1	2500	
MSM81_35-1	3/10/2019 23:35	Sound Velocity Profiler	on deck	50° 13,146' S	046° 51,215' W	2750.1	0	93	300	17.1	EL1	0	

Appendix B Seismic Profile Summary

PROFILE # AWI-…	Start / End	DATE	TIME (UTC)	LATITUDE	LONGITUDE	FFIDs, # of SHOT	RECORD LENGTH (s)	SAMP. RATE (ms)	SHOT INTERVAL (m)	PROFILE LENGTH (nm)	STREAMER	GI-GUN ARRAY		COMMENT
												Set-up	Total volume	
20190001	start end	13.02.19 15.02.19	16:19:00 12:10:00	-52.44701 -50.63975	-50.4805859 -46.0489889	295- 15082	9	1	25	200	SEAL428	4 GI-guns, true GI mode (45+105 in^3), 35 ms delay	4 * 2.4 l	Start of ramp-up 15:08, full power 15:28 Site 511 CDP 11776 Site 330 CDP 12230 Site 327 CDP 12589 Site 329 CDP 14757
20190002	start end	15.02.19 16.02.19	12:48:00 23:24:00	-50.63059 -49.72736	-46.094688 -49.76888	15083- 26317	9	1	25	152	SEAL 428	4 GI-guns, true GI mode (45+105 in^3), 35 ms delay	4 * 2.4 l	
20190003	start end	17.02.19 18:02:19	00:17:00 18:58:00	-49.74087 -52.88667	-49.720725 -47.550443	26394- 41695	9	1	25	207	SEAL 428	4 GI-guns, true GI mode (45+105 in^3), 35 ms delay	4 * 2.4 l	
20190004	start end	18.02.19 19.02.19	20:02:48 21:16:00	-52.8561 -50.83898	-47.572691 -46.769813	41840- 51090	9	1	25	125	SEAL 428	4 GI-guns, true GI mode (45+105 in^3), 35 ms delay	4 * 2.4 l	Site 327 CDP 9177
20190005	start end	19.02.19 21.02.19	22:21:00 03:12:00	-50.87148 -50.90520	-46.783689 -50.55919	51286- 61857	9	1	25	143	SEAL 428	4 GI-guns, true GI mode (45+105 in^3), 30 ms delay	4 * 2.4 l	Site 327 CDP 10
20190006	start end	21.02.19 22.02.19	04:09:00 07:20:00	-50.93502 -52.88299	-50.548286 -49.156888	61858- 70664	9	1	25	119	SEAL 428	4 GI-guns, true GI mode (45+105 in^3), 30 ms delay	4 * 2.4 l	Interruption repairs tow wire 21:20:40 – 23:17:00, soft start
20190007	start end	22.02.19 23.02.19	08:12:00 23:39:19	-47.63156 -46.60909	-49.8157639 -51.3568967	70760- 85129	9	1	25	194	SEAL 428	4 GI-guns, true GI mode (45+105 in^3), 30 ms delay	4 * 2.4 l	

PROFILE # AWI-…	Start / End	DATE	TIME (UTC)	LATITUDE	LONGITUDE	FFIDs, # of SHOT	RECORD LENGTH (s)	SAMP. RATE (ms)	SHOT INTERVAL (m)	PROFILE LENGTH (nm)	STREAMER	GI-GUN ARRAY		COMMENT
												Set-up	Total volume	
20190008	start end	23.02.19 24.02.19	01:19:47 22:25:00	-49.81576 -51.35689	-47.63156 -46.60909	85242- 92772	9	1	25	102	SEAL 428	4 GI-guns, true GI mode (45+105 in^3), 30 ms delay	4 * 2.4 l	Soft start, repairs tow wire 00:39 Site 511 CDP 5693
20190009	start end	24.02.19 26.02.19	22:55:00 02:41:00	-51.38257 -50.31573	-46.654922 -50.008594	92773- 103360	9	1	25	143	SEAL 428	4 GI-guns, true GI mode (45+105 in^3), 30 ms delay	4 * 2.4 l	
20190010	start end	26.02.19 26.02.19	03:16:10 18:00:37	-50.35102 -51.47181	-50.028073 -50.369262	103377- 108469	9	1	25	69	SEAL 428	4 GI-guns, true GI mode (45+105 in^3), 30 ms delay	4 * 2.4 l	
20190011	start end	26.02.19 28.02.19	19:00:00 03:50:00	-51.53559 -52.84153	-50.2948872 -46.340668	108469- 120647	9	1	25	164	SEAL 428	4 GI-guns, true GI mode (45+105 in^3), 30 ms delay	4 * 2.4 l	
20190012	start end	28.03.19 01.03.19	04:47:29 06:13:04	-52.8585 -50.95477	-46.391835 -44.738247	120745- 130361	9	1	25	130	SEAL 428	4 GI-guns, true GI mode (45+105 in^3), 30 ms delay	4 * 2.4 l	
20190013	start end	01.03.19 01.03.19	06:14:08 14:44:42	-50.95339 -50.35810	-44.737031 -44.086398	130365- 133619	9	1	25	44	SEAL 428	4 GI-guns, true GI mode (45+105 in^3), 30 ms delay	4 * 2.4 l	
20970014	start end	01.03.19 02.03.19	15:45:00 13:56:00	-50.33309 -49.90688	-43.981515 -41.258529	133620- 141762	9	1	25	110	SEAL 428	4 GI-guns, true GI mode (45+105 in^3), 30 ms delay	4 * 2.4 l	Soft start, change of buoys Core 33 CDP 1868 Core 13 CDP 4167
20190015	start end	02.03.19 02.03.19	14:35:00 20:00:00	-49.92791 -49.76355	-41.242279 -42.11829	141763- 143789	9	1	25	27	SEAL 428	4 GI-guns, true GI mode (45+105 in^3), 30 ms delay	4 * 2.4 l	Core 16 CDP 1435

PROFILE # AWI-…	**Start / End**	**DATE**	**TIME (UTC)**	**LATITUDE**	**LONGITUDE**	**FFIDs, # of SHOT**	**RECORD LENGTH (s)**	**SAMP. RATE (ms)**	**SHOT INTERVAL (m)**	**PROFILE LENGTH (nm)**	**STREAMER**	**GI-GUN ARRAY**		**COMMENT**
												Set-up	**Total volume**	
20190016	start end	02.03.19 03.03.19	22:35:00 05:51:00	-49.73892 -50.32800	-42.10850 -42.15269	144139- 146764	9	1	25	35	SEAL 428	4 GI-guns, true GI mode (45+105 in^3), 30 ms delay	4 * 2.4 l	Soft start, gun #2 broken
20190017	start end	03.03.19 03.03.19	06:30:00 14:40:00	-50.33475 -49.73970	-42.11554 -42.64591	146765- 149818	9	1	25	35	SEAL 428	4 GI-guns, true GI mode (45+105 in^3), 30 ms delay	4 * 2.4 l	
20190018	start end	03.03.19 03.03.19	15:20:00 21:38:00	-49.73640 -50.21726	-42.59809 -42.921463	149820- 152177	9	1	25	32	SEAL 428	4 GI-guns, true GI mode (45+105 in^3), 30 ms delay	4 * 2.4 l	Core 12 CDP 1040
20190019	start end	03.03.19 04.03.19	22:17:00 04:57:00	-50.21237 -49.74798	-42.87825 -43.34370	152178- 154664	9	1	25	34	SEAL 428	4 GI-guns, true GI mode (45+105 in^3), 33 ms delay	4 * 2.4 l	
20190020	start end	04.03.19 04.03.19	05:34:00 13:40:00	-49.74016 -50.40833	-43.30993 -43.44262	154665- 157694	9	1	25	41	SEAL 428	4 GI-guns, true GI mode (45+105 in^3), 30 ms delay	4 * 2.4 l	Core 33 CDP 2072
20190021	start end	04.03.19 04.03.19	14:17:00 23:46:00	-50.40446 -49.70274	-43.41040 -43.96850	157695- 161236	9	1	25	48	SEAL 428	4 GI-guns, true GI mode (45+105 in^3), 30 ms delay	4 * 2.4 l	
20190022	start end	05.03.19 05.03.19	00:20:00 12:23:00	-49.69599 -50.65957	-43.93575 -44.20467	161238- 165634	9	1	25	59	SEAL 428	4 GI-guns, true GI mode (45+105 in^3), 33 ms delay	4 * 2.4 l	
20190023	start end	05.03.19 06.03.19	13:31:00 02:21:00	- 50.70632 - 49.69969	- 44.17689 - 44.52337	165635- 170262	9	1	25	62	SEAL 428	4 GI-guns, true GI mode (45+105 in^3), 33 ms delay	4 * 2.4 l	
20190024	start end	06.03.19 06.03.19	03:06:00 15:57:48	- 49.69489 - 50.69607	- 44.48473 - 45.06862	170263- 175059	9	1	25	65	SEAL 428	4 GI-guns, true GI mode (45+105 in^3), 30 ms delay	4 * 2.4 l	

PROFILE # AWI-…	Start / End	DATE	TIME (UTC)	LATITUDE	LONGITUDE	FFIDs, # of SHOT	RECORD LENGTH (s)	SAMP. RATE (ms)	SHOT INTERVAL (m)	PROFILE LENGTH (nm)	STREAMER	GI-GUN ARRAY		COMMENT
												Set-up	Total volume	
20190025	start end	06.03.19 07.03.19	17:29:00 06:49:00	- 50.72354 - 49.73679	- 45.05318 - 45.72112	175060- 179882	9	1	25	65	SEAL 428	4 GI-guns, true GI mode (45+105 in^3), 30 ms delay	4 * 2.4 l	
20190026	start end	07.03.19 08.03.19	07:28:00 02:21:00	-49.70803 -51.10833	-45.67803 -46.72581	179883- 186791	9	1	25	93	SEAL 428	4 GI-guns, true GI mode (45+105 in^3), 30 ms delay	4 * 2.4 l	
20190027	start end	08.03.19 08.03.19	03:00:00 10:00:00	-51.11796 -50.54973	-46.68707 -46.88883	186792- 189385	9	1	25	35	SEAL 428	4 GI-guns, true GI mode (45+105 in^3), 30 ms delay	4 * 2.4 l	Site 327 CDP 1124
20190028	start end	08.03.19 08.03.19	10:01:00 19:43:00	- 50.54719 - 49.77101	- 46.88968 - 46.59078	189386- 192940	9	1	25	48	SEAL 428	4 GI-guns, true GI mode (45+105 in^3), 30 ms delay	4 * 2.4 l	
20190029	start end	08.03.19 09.03.19	20:41:00 18:39:00	- 49.80205 - 49.89926	- 46.62181 - 43.70832	192942- 201403	9	1	25	114	SEAL 428	4 GI-guns, true GI mode (45+105 in^3), 30 ms delay	4* 2.4 l	
20190030	start end	09.03.19 10.03.19	19:13:00 19:00:00	-49.87682 -50.16888	-43.69588 -46.60431	201404- 209907	9	1	25	115	SEAL 428	4 GI-guns, true GI mode (45+105 in^3), 30 ms delay	4 * 2.4 l	
									Total length =	2810 nm				